AD-A039 001 PURDUE UNIV LAFAYETTE IND PROJECT SQUID HEADQUARTERS F/G 7/4
HTFFR KINETICS STUDIES OF AL + CO2 YIELDS A10 + CO FROM 300 TO --ETC(U)
APR 77 A FONTIJN, W FELDER N00014-75-C-1143
UNCLASSIFIED SQUID-AC-16-PU NL

| OF |
AD
A039001

END

DATE
FILMED
5-77

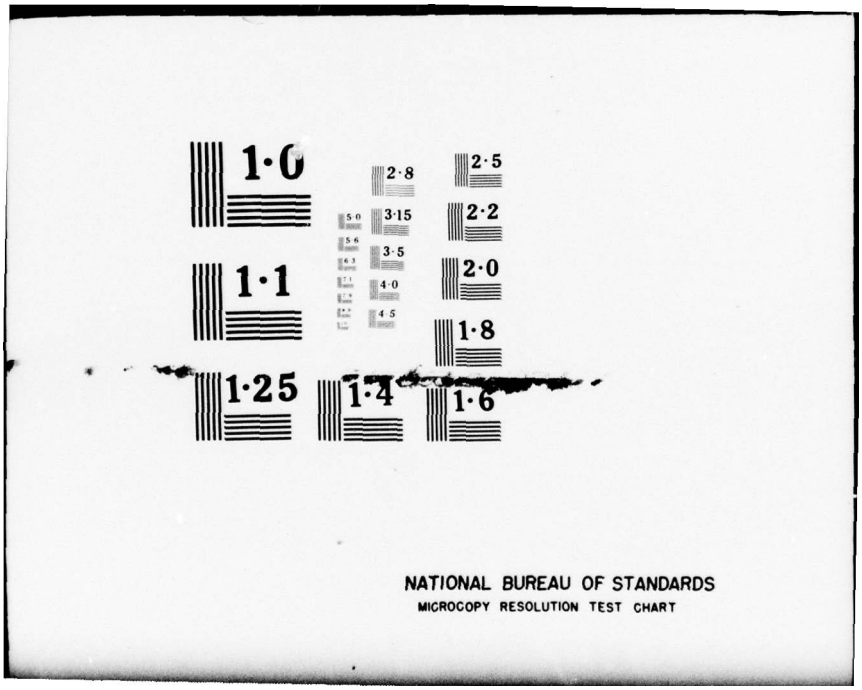
1·0
1·1
1·25
1·4
1·6
1·8
2·0
2·2
2·5
2·8
3·15
3·5
4·0
4·5
5·0
5·6
6·3
7·1
8·0
9·0
NATIONAL BUREAU OF STANDARDS
MICROCOPY RESOLUTION TEST CHART

PROJECT SQUID
TECHNICAL REPORT AC-16-PU

HTFFR KINETICS STUDIES OF $A1 + CO_2 \rightarrow A1O + CO$ FROM 300 to 1800 K, A NON-ARRHENIUS REACTION

BY

ARTHUR FONTIJN AND WILLIAM FELDER
AEROCHEM RESEARCH LABORATORIES, INC.
PRINCETON, NEW JERSEY 08540

PROJECT SQUID HEADQUARTERS
CHAFFEE HALL
PURDUE UNIVERSITY
WEST LAFAYETTE, INDIANA 47907

APRIL 1977

Project SQUID is a cooperative program of basic research relating to Jet Propulsion. It is sponsored by the Office of Naval Research and is administered by Purdue University through Contract N00014-75-C1143, NR-098-038.

(14) SQUID-

(9) Technical Report AC-16-PU

PROJECT SQUID

A COOPERATIVE PROGRAM OF FUNDAMENTAL RESEARCH
AS RELATED TO JET PROPULSION
OFFICE OF NAVAL RESEARCH, DEPARTMENT OF THE NAVY

(6) HTFFR KINETICS STUDIES OF Al + CO_2 → AlØ + CO FROM 300 to 1800 K, A NON-ARRHENIUS REACTION.

by

(10) Arthur Fontijn and William Felder
AeroChem Research Laboratories, Inc.
Princeton, New Jersey 08540

(15) N00014-75-C-1143

(11) April 1977

(12) 36p.

AB

HTFFR kinetics studies of Al + CO_2 → AlO + CO from 300 to 1800 K, a non-Arrhenius reaction*

Arthur Fontijn and William Felder

AeroChem Research Laboratories, Inc.
P.O. Box 12, Princeton, NJ 08540

High-temperature fast-flow reactors (HTFFR) were used to obtain the rate coefficients, k_1 (and their accuracies), for the reaction Al + CO_2 → AlO + CO. At 310, 480, 730, 1470, and 1830 K, k_1 is found to be $(1.5 \pm 0.6) \times 10^{-13}$, $(6.9 \pm 2.7) \times 10^{-13}$, $(1.6 \pm 0.7) \times 10^{-12}$, $(9.0 \pm 3.8) \times 10^{-12}$ and $(3.8 \pm 1.5) \times 10^{-11}$, respectively (all in ml molecule^{-1} s^{-1} units). For this temperature range $k_1(T)$ may be expressed by the curve fitting equation

$$k_1(T) = 2.5 \times 10^{-13} T^{1/2} \exp(-1030/T) + 1.4 \times 10^{-9} T^{1/2} \exp(-14{,}000/T)$$

The data also indicate a wall-oxidation process of zeroth order in [CO_2] with a γ_{Al} of 10^{-3} to 10^{-2}, not measurably dependent on T. Factors affecting the accuracy of the measurements are discussed. Over the 310-730 K range $k_1(T)$ obeys an Arrhenius expression, with an activation energy of 2.6 ± 1.3 kcal mole^{-1}, which implies D(Al–O) $\geq$ 122 kcal mole^{-1}. Above 730 K, $k_1(T)$ increases much more rapidly with T. This behavior cannot be described on the basis of simple transition state theory alone; the most probable additional factors involved are the opening of a second reaction channel leading to AlO($A^2\Pi$) and preferential reaction of Al with CO_2 in bending modes.

---

* Prepared for submission to the Journal of Chemical Physics

I. INTRODUCTION

We have previously described metal atom oxidation studies using a high-temperature fast-flow reactor (HTFFR) which, in its various modifications, allows the measurement of rate coefficients of reactions over roughly the 300-2000 K temperature range. Our earlier HTFFR measurements covered most of this range for the Al/O_2 [2,3] and AlO/O_2 [4,5] reactions. The rate coefficients of both these reactions were found to be, within experimental error, temperature independent.[2] In the present work we have studied the reaction

$$Al + CO_2 \rightarrow AlO + CO \qquad (1)$$

This reaction was selected since, on the basis of the most commonly accepted bond energy of AlO, it is endothermic (by about 5 to 6 kcal $mole^{-1}$) [4,5] and hence has an activation energy, i.e., a temperature-dependent rate coefficient. The reaction has indeed been found here to have a positive activation energy, though evidence is discussed suggesting it may be somewhat more energetic than usually assumed.

II. TECHNIQUE

The HTFFR used in the experiments at $T \geq 730$ K was the 95 cm long single furnace unit previously described[2,3,6] and hereafter referred to as "Reactor 1". Lower temperature experiments with Al necessitated a somewhat different design, since the heat generated by the source at the required Al fluxes is sufficient to generate a reaction zone temperature of ≈ 700 K even when no additional heat is supplied to this zone by the furnace resistance wire. The 300 K modification "Reactor 2", consisting of a high-temperature Al-atom source section and a water-cooled reaction zone, has recently been described.[1] The present work includes experiments at ≈ 480 K for which another modification of the HTFFR, shown schematically in Fig. 1,

had to be developed ("Reactor 3"). (This new reactor was also used for a few consistency checks at 730 K.) The first section of this modular HTFFR consists of a 27 cm long heated (to about 1700 K) source tube in which the Al in Ar "source gas" is generated. As in Reactor 2, this section is followed by a short (≈ 5 cm) non-insulated copper section where additional room-temperature Ar ("main gas") may be introduced. The Al/Ar flow emanates from this section at $T \lessapprox 400$ K and flows into the independently heated reaction tube section. In this section, constructed similarly to the source section, the oxidant CO_2 is introduced through an axially traversable inlet and the relative Al concentration $[Al]_{rel}$ is measured at the observation plane (containing four windows each at 90° from the adjacent windows), using the same arrangements as in the HTFFR versions previously described.[1-3,6] The 20 cm length of the alumina reaction tube to the observation windows can be traversed with the CO_2 inlet.

The source, main and sweeper gas, Fig. 1, was Ar obtained from high purity (99.998% min.) liquid Ar containers. Al was evaporated from Al-wetted tungsten wire sources.[2] Two sources of CO_2 were used: for the slower rates and shorter reaction times, predominantly a "100%" CO_2 cylinder (analyzed to contain 79 ppm O_2 and 80 ppm N_2),[7] and (especially needed because of the increased rate coefficient, at the highest temperatures) a 9.56% CO_2 in Ar cylinder, containing < 2 ppm O_2 and < 4 ppm N_2.[7]

Except at 1830 K, the measurements were made under pseudo first-order conditions, $[CO_2] >> [Al]$, the basic measurement being that of $[Al]_{rel} = [Al]/[Al]_i$ as a function of $[CO_2]$, $[M]$, t and T. Here $[Al]_i$ denotes initial Al concentration in the absence of CO_2, and $[Al]$, the Al concentration at

the observation port after CO_2 addition.[1,2] Either fluorescence or absorption was used to measure $[Al]_{rel}$, using the line radiation from an Al hollow cathode lamp, chopped at 140 Hz. Additionally, prior to CO_2 introduction in each fluorescence experiment, $[Al]_i$ was measured in absorption; thus absorption serves to determine the degree of variation in $[Al]_i$ over all experiments. Al absorption for fluorescence measurements varied from about 3 to 20% (which is in the linear portion of the curve-of-growth); wider variation was obtained where possible by including fluorescence and absorption experiments in the set of measurements at a given temperature; for the latter an initial absorption on the order of 50% was used. Also to allow measurement of as large a variation in $[Al]_i$ as possible, three Al lines of different oscillator strength (309.3 nm, gf = 0.70; 394.4 nm, gf = 0.23 and 396.2 nm, gf = 0.46)[8-10] were used in the absorption experiments. From these gf values, a lamp temperature of 600 K[11] and P = 15 Torr and, assuming Doppler and pressure broadened absorption lines, [Al] is estimated to be 0.9, 1.9 and 1.0×10^{12} ml^{-1} at 1830 K and 1.0, 1.4 and 1.2×10^{12} ml^{-1} at 310 K for 50% absorption at these wavelengths, respectively. In absorption experiments the detector consisted of monochromator/PMT combinations, while for the fluorescence measurements the 309.3 nm line was used with a PMT equipped with a 309.1 nm (11 nm fwhm) interference filter as detector. Above $\approx$ 1500 K absorption was found to be the only practical technique because of the high background radiation from the reaction tube walls. Near 300 K only fluorescence could be used since the source conditions required for the large $[Al]_i$ of absorption experiments led to an increase in the reaction tube temperature above that used in the fluorescence experiments.

As before[2,3] data were obtained using either the traversing oxidant inlet mode (where measured pseudo first-order rate coefficients k_{ps_1} give the reaction rate coefficient k_1 from the slope of plots of k_{ps_1} vs. $[CO_2]$) or the stationary CO_2 inlet mode, which is more facile especially at the higher temperatures. In the latter mode k_1 is obtained directly from plots of $[Al]_{rel}$ vs. $[CO_2]$ for a given inlet position and the measurements are typically repeated at one or two additional positions (including e.g., 20, 12 and 7 cm upstream from the observation ports); the results reported from these stationary inlet measurements are the averages of two or, more commonly, three such experiments. The individual k_1 measurement plots obtained are of similar quality as those of the Al/O_2 work[1,2] (standard deviations of 10 to 20%).

For the k_1 measurements at 1830 K the full bimolecular rate equation had to be used rather than its pseudo first-order approximation,[12] since at the lower part of the $[CO_2]$ range used, $[Al] \approx [CO_2]$. This is due to (i) the large value of k_1 (1830 K) which requires low $[CO_2]$ in order to maintain reasonable reaction rates and (ii) the high [Al] inherent in the use of absorption relative to fluorescence measurements.

III. RESULTS

A. $k_1(T)$ measurements

The k_1 measurements made are summarized in Table I. It may be seen that the data at each of the five nominal temperatures used cover a wide range in pressure, P, average gas velocity, $\bar{v}$, and $[Al]_i$ and are independent of these quantities. In Fig. 2 the mean k_1 and standard deviation for each of these temperatures are plotted in the standard Arrhenius fashion, showing a strong departure from linearity above 730 K with an activation energy

increasing with T. To establish an analytical description of this temperature dependence least squares fits to several functional expressions for $k_1(T)$ were tried. The procedure followed was similar to that followed by Bemand, Clyne and Watson[13] and consisted of assigning equal weights to all of the 62 data points of Table I and fitting these to expressions (A)-(D) below. The polynomials (A)-(C) were fit to successively higher degrees from 1 up to p = 4, q = 4, and r = 3, respectively, using linear multiple regression techniques,[14] while expression (D) was fit using Marquardt's method[14] for s = 0 and 1/2:

$$\left.\begin{aligned} \ln k_1(T) &= \ln A_o + A_p/T^p \\ \ln k_1(T) &= \ln A'_o + 0.5(\ln T) + A'_p/T^p \end{aligned}\right\} \quad \text{Arrhenius form} \qquad (A), (A')$$

$$\ln k_1(T) = \ln B_o + B_q(\ln T)^q \qquad T^n \text{ form} \qquad (B)$$

$$\ln k_1(T) = \ln C_o + C_1(\ln T) + C_r/T^r \qquad \text{Transition state theory form} \qquad (C)$$

$$k_1(T) = D\,T^S \exp(-E/T) + F\,T^S \exp(-G/T) \qquad \text{Double exponential form} \qquad (D)$$

At each increase of p, q, and r above zero, the computed fit was examined using the F-test for significance.[14] Comparisons among the various fits were made using the computed value of χ^2 such that the best fit was determined as that functional form which yielded the smallest χ^2 value. The best overall fit (minimum χ^2 value) was obtained from expression (D) with s = 1/2, while for each of the polynomials, (A)-(C), the maximum significant degree (F-test) was p = q = r = 1. Standard deviations, based on random errors only (see Sec. III.C for discussion of systematic errors) were then determined for the computed fitting expressions. The following results were obtained from (A) through (D), respectively, for the temperature dependence of k_1 (fitting error limits = 2σ):

$$\ln k_1(T) = (-24.03 \pm 0.39) - (1830 \pm 170/)T \qquad (E)$$

$$\chi^2 = 0.373$$

$$\ln k_1(T) = (-27.88 \pm 0.34) + 0.5 \ln T - (1500 \pm 150)/T \qquad (E')$$

$$\chi^2 = 0.309$$

$$\ln k_1(T) = (-45.31 \pm 1.48) + (2.76 \pm 0.16) \ln T \qquad (F)$$

$$\chi^2 = 0.162$$

$$\ln k_1(T) = (-47.55 \pm 7.10) + (3.05 \pm 0.69) \ln T + (204 \pm 4740)/T \qquad (G)$$

$$\chi^2 = 0.163$$

$$k_1(T) = (2.48 \pm 1.71) \times 10^{-13} T^{1/2} \exp[(-1032 \pm 410)/T] + (1.41 \pm 0.72) \times 10^{-9} T^{1/2} \exp[(-13989 \pm 1800)/T] \qquad (H)$$

$$\chi^2 = 0.08$$

Figure 3 shows a plot of the fitting functions computed compared to the data obtained. Expressions (F) and (G) give essentially identical curves. All of the forms tested, except the double exponential, (H), fail to attain the large value for k_1 observed at 1830 K. Expression (H), which is a convenient form for use in kinetic modeling studies, represents the best fit to the data obtained and is the recommended expression for $k_1(T)$; higher degree polynomials than those given above in expressions (E)-(G) result in oscillations in $k_1(T)$ which cause the fitting expressions to exhibit physically unrealistic local maxima and minima in regions of the 310-1830 K range where no data were obtained. This latter fact, as well as the statistical significance tests applied are reasonable grounds for rejecting polynomials of degree greater than unity.

B. Wall oxidation coefficient

As in the earlier HTFFR measurements, the plots from which the homogeneous rate coefficients are obtained have positive intercepts. In a limited number of experiments the k_{wall} values are less than the calculated diffusion limited values allowing calculation of a wall oxidation coefficient, γ_{Al}.[2,15] The γ_{Al} thus obtained (and their standard deviations) are in units of 10^{-3}; 1.9 ± 1.4[2], 5.8 ± 1.8[4], 6.2 ± 4.2[4], 12.7 ± 8.3[5], and 4.5 ± 4.0[8] at 310, 480, 730, 1470, and 1830 K, respectively; here the numbers in brackets signify the number of experiments from which γ_{Al} was obtained at each temperature. Within the scatter of these data no definite temperature dependence is evident. Combining all γ_{Al} measurements leads to a value $\gamma_{Al} = (7.7 \pm 6.8) \times 10^{-3}$, i.e., γ_{Al} can be taken to be in the 1×10^{-3} to 1×10^{-2} range. This γ pertains to oxidation on oxide coated walls on an alumina (470-1830 K) or copper (300 K) substrate. This continuous formation of non-volatile Al oxide coatings on the walls in the course of the experiments is in itself probably the factor responsible for the large scatter in the γ_{Al} measurements, i.e, is responsible for variation in wall reactivity.

C. Accuracy of the $k_1(T)$ measurements

1. Concentrations and time

The uncertainty in k_1 due to inaccuracy in the volume flow rate, pressure and temperature (discussed in Sec. III.C.2) measurements is estimated to be ± 20%. Additionally, at the flow conditions used, selected to give (i) adequate Al transport and (ii) acceptable temperature accuracy (see Sec. III.C.2), the flow profiles are calculated to be intermediate between plug and parabolic flow. If the former condition had prevailed (the criteria for which have been developed by Walker[16,17]) η in the expression $t = x/\eta\bar{v}$

would have been 1.0. If the latter had prevailed, for the development of which inadequate distance is available,[18,19] $\eta = 1.6$. For this reason we have again[1-3,15] taken $\eta = 1.3$ ($\pm$ 0.3 = 23%) for the k_1 calculations.

The question arises whether higher accuracy would be achievable if η were calculated for each individual experiment. However, in the intermediate flow regime of the experiments no analytical solution apparently is possible, nor does it seem likely that a numerical treatment (similar in kind to that of Ref. 18) would be helpful since inspection of Table I shows that the scatter in the k_1 values obtained under nearly identical flow conditions is comparable to that which pertains at widely different conditions. The reasons for this are probably related to the high somewhat variable wall reactivity and the (thin) metal oxide deposits along the reactor walls. In this light, taking a separate error factor of $\pm$ 23% for η may lead to an overestimate in the combined uncertainty factor, since the same factor must to some degree be reflected in the data scatter, However, it can readily be seen (by estimating the accuracy of k_1 using the usual procedure of taking the square root of the sum of the squares of the individual error estimates)[1-3, 15] that the contribution of this 23% factor on top of the discussed 20% systematic error and the 25 to 30% standard deviation (cf. Table 1) is minor. (Slight overestimation of errors is probably the most forgivable of sins.)

It is interesting to note that, in flow tube studies of non-refractory species such as O, N, H, or halogen atoms, rate coefficient accuracies in the range of 10-20% are readily obtainable, especially at room temperature (see e.g., Refs. 20-23). The major differences between those studies and the present flow tube work with refractory species are that in the former plug flow conditions are readily obtained ($\eta = 1$ within 5%)[17,24,25] and γ can be kept

small (on the order of 10^{-5} at 300 K)[25] and constant.[26] However, some of the temperature inaccuracies discussed below are also present at temperatures other than room temperature in those (and other) kinetic studies, though they often appear to go unrecognized.

2. Temperature

Because of the strong and interesting temperature dependence of k_1, a careful reexamination of the accuracy of the temperature determinations has been made. Temperature is measured with a Pt/Pt-10% Rh thermocouple (TC), attached to the CO_2 distributor ring[6] and situated 0.5 cm from the reactor wall. The leads to the TC junction are fed through a two-hole alumina "thermocouple tube" and the junction itself is covered with alumina paste. For the conditions of this work (Mach number ≤ 0.2; Reynolds number with respect to the reaction tube diameter ≤ 2300 at 310 K, ≤ 1000 at the other temperatures; Reynolds numbers with respect to the coated thermocouple diameter ≈ 0.13 times those for the reaction tube) radiative heat transfer between the TC junction and the reactor walls is the potential major source of systematic uncertainty.[27] As a first step in evaluating the significance of this factor calculations were made of axial and radial temperature distributions for unobstructed laminar flow of Ar in a uniformly heated HTFFR by solving the Graetz equation.[28,29] The flow conditions used, Table I, are found to satisfy the criteria that the calculated mean gas temperature at the upstream boundary of the reaction zone be within 5% of the nominal wall temperature and that the extremes of radial temperature variation be within 5% of this mean temperature. The actual variations are undoubtedly smaller for the following reasons: (i) laminar, unobstructed flow is assumed in the calculation, whereas the Al source and its support tube (Fig. 1 and Ref. 6) leave

only a small flow path in the source area, which increases thermal contact with the walls, (ii) flow development with reaction time aids the establishment of thermal equilibrium between the gas and walls, and (iii) the simplified model does not take into account the capability of the three heating zones[6] of Reactor 1 to produce an upstream zone at a higher temperature than the reaction zone, i.e., to allow preheating of the Al/Ar flow. Thus on this basis, the temperature measurement error would be considerably less than 5%. Indeed, measurements were made comparing centerline and offset (to the position used in the experiment) TCs showing that radial temperature gradients are negligible (centerline and offset temperatures agree to $\approx$ 0.1% of $\bar{T}$). (Interestingly, when the source tube was removed radial temperature gradients increased to as much as 5% of $\bar{T}$.)

Direct evidence that radiative heating is not causing an overestimate of T is the consistent observation that when the bath Ar flow is turned off at the end of an experiment the indicated reaction zone temperature decreases, which shows that the gas is hotter than the walls. As an additional check, experiments were carried out in which the HTFFR centerline temperatures were obtained simultaneously from two TCs: one similar to those used in the rate coefficient measurements and the other, 5 cm upstream, an identical TC shielded[27] by placing it in the center of a 6 cm long, 1.8 cm o.d., 1.2 cm i.d. alumina (open-ended) cylinder. Comparisons were performed for typical experimental conditions near 730 and 1470 K. In all cases the shielded TC tended to indicate slightly higher temperatures, thus some radiative cooling of the TCs used in the rate coefficient measurements occurred. However, in all cases the agreement between the two TCs was within 5% and was best at low pressure (3 Torr) and at 1470 K.

Additionally, for measurements obtained with modular Reactor 2 significant falsification of the TC readings can be ruled out since varying the fraction of bath gas (Ar) which flowed into the reactor through the source, Fig. 1 (temperature near 1700 K) between 1.0 and 0.03 had no apparent effect on the measured k_1 values (the remainder, i.e., the "main gas" entered the reactor at room temperature). Because of the temperature dependence of k_1 some effect of these flow variations would have been observed if the reaction zone temperature had varied significantly. Thus $\overline{T}$ was essentially the same in all the "310 K" measurements and must have been close to this temperature since the gas mixture in the case where 97% of the Ar entered the reactor at room temperature could not have achieved a significantly higher $\overline{T}$. Similarly, no influence of varying the main to source gas flow ratio on the k_1 measurements with Reactor 3 could be observed.

In addition to these considerations indicating systematic errors to be $\leq$ 5%, the precision of the $\overline{T}$ measurements has to be considered. $\overline{T}$ values of the individual experiments of Table I are the averages of the T measurements over the useful length of the reaction zone.[15] The standard deviation, of the T at the various CO_2 inlet positions, from $\overline{T}$ was 2 to 3%. Thus the uncertainty of the T measurements of the individual experiments is $\leq [(5.0)^2 + (2.5)^2]^{1/2} = 5.6\%$. To determine the accuracy of the $\overline{T}$ for the set of experiments at a given nominal temperature, the standard deviation of the set of $\overline{T}$ measurements should be taken into account. Inspection of Table I shows that this factor varies from 1 to 4% and thus contributes only slightly to the cumulative uncertainty; $\leq$ 6% may be taken as the approximate uncertainty figure for general $\overline{T}$ considerations.

3. The 1830 K rate coefficient measurements

At equilibrium at 1830 K, CO_2 is appreciably dissociated at the partial pressures of interest. We have calculated the effect such dissociation could have had on the k_1 (1830 K) measurements by using an AeroChem thermodynamic equilibrium computer code and JANAF[4] log K_p data. The principal dissociation products are CO and O_2, with only minor amounts (< 0.05 $[O_2]$) of O atoms and no other products (C_2O and C_3O_2 were considered) present. Because of its strong bond ($D(C{-}O) \approx 260$ kcal mole^{-1}) CO could react with Al only in a three-body process, of which there is no evidence in the data (k_1(1830 K) does not increase with P). However the O_2 from the equilibrium

$$CO_2 \rightleftarrows CO + 0.5\ O_2 \qquad (2)$$

will react with Al. For the reaction

$$Al + O_2 \rightarrow AlO + O \qquad (3)$$

we previously determined[1,2] (in the same apparatus) a rate coefficient of $(3.4 \pm 2.2) \times 10^{-11}$ ml molecule^{-1} s^{-1}. Thus if CO_2 would have been completely dissociated, an apparent $k_1 = 0.5\ k_3$ would have been observed, lower than the actual k_1 measurements. The calculated fractional equilibrium dissociation $\alpha = 1 - [CO_2]/[CO_2]_o$ (where $[CO_2]_o$ is the $[CO_2]$ before dissociation or reaction) varies over the range of $[CO_2]_o$ used in the experiments, from 0.57 at $[CO_2]_o = 1 \times 10^{12}$ ml^{-1} to 0.07 at $[CO_2]_o = 1 \times 10^{15}$ ml^{-1}. Using these numbers the actual observations were then "corrected" by obtaining k_1 values from plots of the following equations (compare Ref. 2):

$$\text{Stationary:}\quad -\ln[Al]_{rel}^{corr} = -\ln[Al]_{rel}^{obs} - k_3[O_2]t = k_1[CO_2]t + k_{wall}t$$

$$\text{Traversing:}\quad k_{ps_1}^{corr} = k_{ps_1}^{obs} - k_3[O_2] = k_1[CO_2] + k_{wall}$$

The mean of the k_1 thus obtained was found to be 6% higher than that of Table I. Thus while CO_2 dissociation could contribute somewhat to the uncertainty in k_1(1830 K) this effect appears minor compared to the standard deviation (Table I) and error factors already discussed (Sec. III.C.I). There is moreover no evidence that equilibrium dissociation was achieved. Such is in fact unlikely on the basis of the observations that (i) there are no trends in the individual $[Al]_{rel}$ (or k_{ps_1}) plots versus CO_2 which indicate consistent deviations from linearity and (ii) a few stationary inlet measurements made at a measured T of $\approx$ 1900 K (representing the approximate maximum safe operating temperature of the HTFFR) indicated a somewhat lower k_1 than that obtained at 1830 K, which moreover decreased with increasing reaction time, indicative of CO_2 dissociation at that temperature and negligible dissociation at 1830 K.

4. Recommended k_1 values

For k_1 at each of the five nominal temperatures of Table I the uncertainty can now be obtained by taking the square root of the sum of the squares of the individual error assessments, which thus consist of the standard deviations and the 20% and 23% factors of Sec. III.C.1. Taking the temperature accuracy as $\pm$ 6%, cf. Sec. III.C.2, we thus obtain from Table I:

$$k_1(310 \pm 20\ K) = (1.5 \pm 0.6) \times 10^{-13}\ ml\ molecule^{-1}\ s^{-1}$$

$$k_1(480 \pm 30\ K) = (6.9 \pm 2.7) \times 10^{-13}\ ml\ molecule^{-1}\ s^{-1}$$

$$k_1(730 \pm 40\ K) = (1.6 \pm 0.7) \times 10^{-12}\ ml\ molecule^{-1}\ s^{-1}$$

$$k_1(1470 \pm 90\ K) = (9.0 \pm 3.8) \times 10^{-12}\ ml\ molecule^{-1}\ s^{-1}$$

$$k_1(1830 \pm 110\ K) = (3.8 \pm 1.5) \times 10^{-11}\ ml\ molecule^{-1}\ s^{-1}$$

To obtain k_1 at any other temperature, Equation (H) of Sec. III. A should be used to obtain the mean value and experimental error. The accuracy can then

be obtained by combining this error with the 20% and 23% factors, as above.

D. The lower limit to D(Al—O)

While Reaction (1) has a strongly curved Arrhenius plot, Figs. 2 and 3 show that, over the 310 to 730 K range, $k_1(T)$ adheres quite well to Arrhenius behavior with an activation energy $E_{act}(1) = 2.6 \pm 1.3$ kcal mole^{-1}; these error limits reflect the discussed precision and possible systematic inaccuracy sources in both k_1 and T. Since $\Delta H(1) \leq E_{act}(1)$, Reaction (1) can at most be 3.9 kcal endothermic; if the classical $T^{0.5}$ factor in the pre-exponential had been included in the calculation (which procedure may not be justifiable in view of e.g., the T^0-dependence of the rate coefficients of the Al/O_2 and AlO/O_2 reactions)[1] an even smaller endothermicity would have resulted. Using JANAF ΔH (individual species) values[4] a $\Delta H(1)$ of 6.0 and 5.8 kcal mole^{-1} is calculated at 300 and 800 K, respectively. The JANAF data are based on $D(Al—O) = 120 \pm 2$ kcal mole^{-1} and only this upper limit would thus be within the range allowed by the measured $E_{act}(1)$ values. Since endothermic reactions usually have an activation energy at least somewhat higher than their ΔH this finding thus casts some doubt on the JANAF D(Al—O) value. Dagdigian, Cruse and Zare[5] have recently determined a lower limit to D(Al—O) and combining their value with an evaluation of the literature for the upper limit, they recommend $D(Al—O) = 121.5 \pm 1$ kcal mole^{-1}, accepting essentially the same upper limit as JANAF. However, improved laser fluorescence experiments by Dagdigian and Pasternack,[30] now in progress, using a velocity selected Al beam[31] lead them to recommend $D(Al—O) = 123.0 \pm 1$ kcal mole^{-1}. Flame photometric data, notably Ref. 32, also tend to indicate higher D(Al—O) values. Those determinations are dependent on the f-number of the AlO(B—X) transition, which has been determined accurately in the same work of Dagdigian, Cruse and Zare.[5] Using this f number the

data of Ref. 32 reduce[33] to D(Al—O) = 132 ± 6 kcal mole^{-1}. On the basis of all these data we conclude that D(Al—O), and hence ΔH of Reaction (1), may not yet be accurately known and consider it probable that D(Al—O) is a few kcal mole^{-1} larger than 122. We are presently measuring the activation energy of a reaction of Al with an oxidizer having an O atom more strongly bonded than in O—CO, i.e., O—SO, in an attempt to help clarify this problem.

IV. DISCUSSION

The present work represents the first time that a reaction having a definite activation energy has been measured from near room temperature to a "high" temperature such as 1800 K, by a single technique. Over such a wide T-range some deviation from Arrhenius behavior may be anticipated, since the simplifying approximations on which the Arrhenius law is based become quite inaccurate.[34,35] Such deviation can be especially strong for reactions having low activation energies, such as Reaction (1) where the temperature-dependence of the entropy of activation can become the dominating factor in the k_1-T dependence. The strong deviation from Arrhenius behavior here observed thus is remarkable but certainly not unprecedented; for example, some reactions of OH[20,36-38] and O[39] show somewhat similar behavior and have been thoroughly discussed. In fact,[40] in the sense that Al may be considered an H substitute, Reaction (1) is the reverse of what is now a classical case of such behavior, viz. the reaction OH + CO → CO_2 + H.[20,36,38,41]

Transition state theory (TST) probably offers the most general promise to describe non-Arrhenius behavior. However, as in the case of the Al/O_2 and AlO/O_2 reactions,[1] TST is of little predictive help at present for simple metathesis reactions of metallic species. Figure 3 shows that the best fit to a TST form (curve G) is inadequate to describe the high

temperature behavior of k_1. It is certainly possible to a posteriori assemble a set of assumptions to rationalize the $T^{2.5}$ dependence of k_1 indicated by the curve G equation (Sec. III.A). From TST the pre-exponentials A for the linear and bent intermediate complexes are:

$$A\ (\text{linear}) = C_\ell T^{-0.5} \prod_{i=1}^{6}\left(1 - \exp(-h\nu_i^{\ddagger}/kT)\right)^{-1} \Big/ \prod_{i=1}^{4}\left(1 - \exp(-h\nu_i^{CO_2}/kT)\right)$$

$$A\ (\text{bent}) = C_b \prod_{i=1}^{5}\left(1 - \exp(h\nu_i^{\ddagger}/kT)\right)^{-1} \Big/ \prod_{i=1}^{4}\left(1 - \exp(-h\nu_i^{CO_2}/kT)\right)^{-1}$$

where C_ℓ and C_b are the lumped, temperature-independent constants arising from translational, rotational, and vibrational partition functions of the reactants and the transition state. At 1830 K only the ν_2 mode of CO_2 is in the high temperature limit ($h\nu_2 \ll kT$) under which condition A (linear) $\propto T^{2.5}$ and A (bent) $\propto T^2$ if the transition state vibrations were also at their high temperature limits. However, it appears likely that this state will have high energy stretching modes that do not fulfill the $h\nu_i^{\ddagger} \ll kT$ condition at this temperature which would result in a decreased T-dependence. Since no information is available on the vibrational levels of the postulated intermediates further speculation does not appear productive. As Benson[42,43] has pointed out activation energies for metathesis reactions are not yet well understood and a large experimental data base on sets of similar reactions is required to predict activation energies from TST-based empiricism. For metal oxidation reactions such a data base is not yet available; the present work and that of Ref. 1 hopefully represent one of the first pieces of information from which it may eventually be constructed.

Thus additional factors need be considered to "explain" the observed k_1-T behavior. Expression (H) of Sec. III.A and Fig. 3, which gives the best fit to the data, is the type of expression which arises from complex processes, e.g., the opening of a second product channel at high temperature, or the increased participation of excited reagent states as the population of these states increases with T. The first term of Equation (H) describes the discussed (Sec. III.D) low temperature Arrhenius behavior quite well; however, the pre-exponential of the second term is unrealistically high and suggests that this term is useful merely as a curve-fitting expression and appears to result from more than one such additional process participating at high temperature.

A possible second product channel would be the formation of $AlO(A^2\Pi)$, which lies[44] 15.1 kcal $mole^{-1}$ above $AlO(X^2\Sigma)$ and thus would require an activation energy $\geq$ 15.1 kcal $mole^{-1}$, cf. Equation (H). With regard to increased participation of excited reagent states, it is now well established that vibrational excitation can lead to major increases in rate coefficients and make additional reaction channels accessible, e.g. Refs. 45, 46. Menzinger et al[47,48] have shown that cross sections of some metal atom/N_2O reactions are enhanced by vibrational excitation of N_2O and have made it plausible that the bending mode ν_2 is responsible for these observations. Their[47,48] postulated mechanism is initial electron transfer from the metal atom to N_2O forming an ion pair, i.e., a harpooning type mechanism, which processes often have high (on the order of 3×10^{-9})[49] pre-exponentials. Since ground state linear N_2O has a negative electron affinity but this affinity increases as the molecule is bent (N_2O^- has a bent ground state), the observed cross section increases with [N_2O, $\nu = 2$]. For the iso-electronic species CO_2

which has similar configurations for the neutral and negative ion ground states,[50] increased [CO_2, $\nu = 2$] could similarly increase the observed k_1. In fact, while formation of CO_2^- by electron attachment to ground state CO_2 is prevented by the difference in structure, the work of Cooper and Compton[51] on gas phase reactions between Cs atoms and organic molecules containing bent CO_2 supplies evidence for the ready formation of CO_2^- in reactions involving such CO_2. The total population of CO_2 bent states can be shown, using data from Herzberg,[52] to increase by a factor of 10 over the 310 to 1830 K. Thus it appears likely that excitation of specific vibrational states of CO_2 can contribute to the rapid increase in k_1, but this factor cannot quantitatively be evaluated in the absence of information on the reactivity of CO_2 in such states. Finally, excited electronic states of Al are not significantly populated at the temperatures covered in this work, while the two low-lying spin-orbit states $^2P_{1/2}$ and $^2P_{3/2}$ are both significantly populated at all temperatures covered (at 300 K Al vapor is 45.4% $^2P_{1/2}$ and 53.6% $^2P_{3/2}$ while at 1800 K Al is 35.1% $^2P_{1/2}$ and 64.9% $^2P_{3/2}$) so that no major effect on the reaction rate can arise from them.

V. CONCLUSIONS

One of the major objectives in the development of the HTFFR technique was to allow kinetic measurements from near 300 K to near 2000 K by a single experimental technique, thereby overlapping the temperature domain of traditional near room temperature techniques with that of traditional high temperature techniques such as flames and shock tubes. The present work represents the first time that this objective has been attained for a reaction having a definite activation energy. Over the low temperature (310-730 K) part of the ln k_1 vs. T^{-1} plot Arrhenius behavior is found to be followed. The

activation energy derived from this straight part of the plot (≤ 4 kcal mole^{-1}) has been shown (Sec. III.D) to be only barely compatible with the upper limit (122 kcal mole^{-1}) to D(Al—O) often assumed. At $T > 730$ K, k_1 is found to increase much more rapidly than the Arrhenius law would indicate; this is probably (Sec. IV) due to a combination of factors including, in addition to the entropy of activation factor inherent in transition state considerations, the likely participation of a second reaction channel leading to $AlO(A^2\Pi)$ and/or preferential reaction of Al with CO_2 in bending modes. A definitive quantitative explanation of the T-dependence of k_1 could probably only be made if state-to-state experiments on the Al/CO_2 reaction at the right interaction energies were available. Since k_1 cannot reasonably be expected to rise by more than an order of magnitude with further increases in T, it would be interesting to see an extension of the present measurements to even higher temperatures (under conditions where $[CO_2]$ is accurately known) by traditional high temperature techniques. The overlapping temperatures for such work provided here can be used as check points for those measurements.

ACKNOWLEDGMENTS

We thank J.J. Houghton, R.L. Revolinski, and R. Ellison for capably carrying out the experimental work, W.R. Frenchu for computational assistance, Dr. W.J. Miller (AeroChem), Dr. N.M. Laurendeau (Purdue University), Dr. D.E. Rosner (Yale University), and Dr. R.N. Zare (Columbia University) for helpful discussions, and Dr. D.E. Jensen (Rocket Propulsion Establishment, Westcott, England) and Dr. P.J. Dagdigian (Johns Hopkins University) for sending us material prior to its publication.

REFERENCES

* This work relates to the Department of the Navy Contract N00014-75-C-1143, issued by the Office of Naval Research under Contract Authority NR 098-038. However, the content does not necessarily reflect the position or the policy of the Department of the Navy or the Government, and no official endorsement should be inferred.

1. A. Fontijn, W. Felder, and J.J. Houghton, Sixteenth Symposium (International) on Combustion (The Combustion Institute, Pittsburgh, to be published).
2. A. Fontijn, W. Felder, and J.J. Houghton, Fifteenth Symposium (International) on Combustion (The Combustion Institute, Pittsburgh, 1975), p. 775; Chem. Phys. Lett. 27, 365 (1974).
3. W. Felder and A. Fontijn, J. Chem. Phys. 64, 1977 (1976).
4. JANAF Thermochemical Tables, Dow Chemical Company, Midland, MI, continuously updated.
5. P.J. Dagdigian, H.W. Cruse, and R.N. Zare, J. Chem. Phys. 62, 1824 (1975).
6. A. Fontijn, S.C. Kurzius, J.J. Houghton, and J.A. Emerson, Rev. Sci. Instr. 43, 726 (1972).
7. Analyses performed and mixture prepared by M.G. Scientific, Somerville, NJ.
8. W.L. Wiese, M.W. Smith, and M.B. Miles, Atomic Transition Probabilities, NSRDS-NBS 22, October 1969.
9. W.H. Smith and H.S. Liszt, J. Opt. Soc. Am. 61, 938 (1971).
10. C. Froese Fischer, Can. J. Phys. 54, 740 (1976).
11. H.C. Wagenaar, I. Novotny, and L. de Galan, Spectrochim. Acta 29B, 301 (1974).

12. Pseudo first-order treatment of the 1830 K data yielded a $k_1 = (3.3 \pm 0.7) \times 10^{-11}$, only slightly lower than the k_1 calculated by the full bimolecular treatment, Table I.

13. P.P. Bemand, M.A.A. Clyne, and R.T. Watson, JCS Farady II 70, 564 (1974).

14. P.R. Bevington, Data Reduction and Error Analysis for the Physical Sciences (McGraw Hill, New York, 1969), Chap. 9.

15. A. Fontijn, S.C. Kurzius, and J.J. Houghton, Fourteenth Symposium (International) on Combustion (The Combustion Institute, Pittsburgh, 1973), p. 167.

16. R.E. Walker, Phys. Fluids 4, 1211 (1961).

17. A.A. Westenberg, Twelfth Symposium (International) on Combustion (The Combustion Institute, Pittsburgh, 1969), p. 287.

18. E.E. Ferguson, F.C. Fehsenfeld, and A.A. Schmeltekopf, Advances in Atomic and Molecular Physics 5, 1 (1969).

19. In some experiments fully developed parabolic flow should have been achieved according to the idealized formula for a straight tube[18] $d_p = 0.227rRe$ where r = tube radius and Re = Reynolds number (in terms of the parameters given in Table I, $d_p = C(T)P\bar{v}$, where C(T) is a temperature dependent constant). However, because of such complicating factors as the presence of the Al-atom source, the CO_2 inlet ring and the main gas inlet, Fig. 1, and the non-smooth walls due to buildup of (thin) metal oxide deposits, it is doubtful if this condition was actually obtained.

20. A.A. Westenberg and N. deHaas, J. Chem. Phys. 58, 4061 (1973).

21. A.A. Westenberg and N. deHaas, J. Chem. Phys. 47, 1393 (1967).

22. J.G. Anderson, J.J. Margitan, and F. Kaufman, J. Chem. Phys. 60, 3310 (1974).

23. D.W. Trainor, D.O. Ham, and F. Kaufman, J. Chem. Phys. 58, 4599 (1973).

24. R.E. Huie and J.T. Herron, Prog. Reaction Kinetics 8, 1 (1975).

25. M.A.A. Clyne, Physical Chemistry of Fast Reactions, Vol. 1, edited by B.P. Levitt (Plenum Press, New York, 1973), Chap. 4.

26. The other extreme (fully-developed parabolic flow; $\gamma = 1$) usually obtains in flowing-afterglow studies of ion-molecule reactions, but there, wall losses, though large, are constant rate processes and accuracies to within 20-30% are often obtained; see e.g. A.L. Farragher, Trans. Faraday Soc. 66, 1411 (1970) and C.J. Howard, H.W. Rundle, and F. Kaufman, J. Chem. Phys. 53, 3745 (1970).

27. R.J. Moffat, Temperature: Its Measurement and Control in Science and Industry, Vol. 3, Part 2, edited by A.I. Dahl (Reinhold, New York, 1962), Chap. 52.

28. E.R.G. Eckert and R.M. Drake, Jr., Heat and Mass Transfer, Second Edition (McGraw Hill, New York, 1959), Sect. 7-7.

29. Transport properties for Ar required as input to this calculation were obtained from R.S. Brokaw, "Alignment Charts for Transport Properties; Viscosity, Thermal Conductivity and Diffusion Coefficients for Nonpolar Gases and Gas Mixtures," NASA TR-R-61 (1960).

30. P.J. Dagdigian and L. Pasternack, Private communication, February 1977.

31. L. Pasternack and P.J. Dagdigian, Rev. Sci. Instr. 48, 226 (1977).

32. D.E. Jensen and G.A. Jones, JCS Faraday I 68, 259 (1972).

33. D.E. Jensen, Rocket Propulsion Establishment, Westcott, England, Private communication, April 1976.

34. J.R. Hulett, Quart. Rev. (London) 18, 227 (1964).

35. M. Menzinger and R. Wolfgang, Angew. Chem. Int. Edit. 8, 438 (1969).

36. F. Dryer, D. Naegeli, and I. Glassman, Combust. Flame 17, 270 (1971).

37. W.T. Rawlins and W.C. Gardiner, Jr., J. Chem. Phys. 60, 4676 (1974).

38. I.W.M. Smith and R. Zellner, JCS Faraday II 69, 1617 (1973).

39. D.L. Singleton and R.J. Cvetanovic, J. Am. Chem. Soc. 98, 6812 (1976).

40. P. Gray, Comment in Ref. 1.

41. J.E. Spencer, H. Endo, and G.P. Glass, Sixteenth Symposium (International) on Combustion (The Combustion Institute Pittsburgh, to be published).

42. S.W. Benson, Int. J. Chem. Kin. Symp. 1, 359 (1975).

43. S.W. Benson, D.M. Golden, R.W. Lawrence, R. Shaw, and R.W. Woolfolk, Int. J. Chem. Kin. Symp. 1, 399 (1975).

44. J.K. McDonald and K.K. Innes, J. Mol. Spectry. 32, 501 (1969).

45. M.J. Kurylo, W. Braun, C.N. Xuan, and A. Kaldor, J. Chem. Phys. 62, 2065 (1975).

46. D.J. Douglas, J.C. Polanyi, and J.J. Sloan, Chem. Phys. 13, 15 (1976).

47. D.J. Wren and M. Menzinger, J. Chem. Phys. 63, 4557 (1975).

48. D.J. Wren, A. Yokozeki and M. Menzinger, Electronic Transition Lasers, edited by J.I. Steinfeld (MIT Press, Cambridge, MA, 1976), Sect. I.14.

49. D.R. Herschbach, Adv. Chem. Phys. 10, 319 (1966).

50. M. Krauss and D. Neumann, Chem. Phys. Lett. 14, 26 (1972).

51. C.D. Cooper and R.N. Compton, Chem. Phys. Lett. 14, 29 (1972); J. Chem. Phys. 59, 3550 (1973).

52. G. Herzberg, Molecular Spectra and Molecular Structure. II. Infrared and Raman Spectra of Polyatomic Molecules (Van Nostrand, New York, 1945), p. 274.

TABLE I. Summary of Al + CO_2 → AlO + CO measurements

Mode[a]	P (Torr)[b]	$\bar{v}$ (m s^{-1})	$[Al]_i$ (% abs.)[c]	$[CO_2]$ (10^{15} ml^{-1})	$\bar{T}$ (K)	k_1 (10^{-13} ml $molecule^{-1}$ s^{-1})
Reactor 2, 310 K nominal						
TF309.3	3.0	10	6	0.25 - 1.0	300	2.0
TF309.3	3.3	27	18	1.6 - 4.6	310	1.3
TF309.3	3.5	44	20	2.5 - 7.8	320	2.0
TF309.3	10	11	14	0.18 - 1.9	300	1.6
TF309.3	11	29	4	1.0 - 3.2	310	1.4
TF309.3	11	47	13	1.1 - 5.0	310	1.6
TF309.3	20	10	4	0.9 - 1.6	310	1.8
TF309.3	21	29	4	0.8 - 6.1	310	1.0
TF309.3	21	48	11	0.7 - 6.4	320	1.1
				Avg.[d]	310 ± 10	1.5 ± 0.4

Mode[a]	P (Torr)[b]	$\bar{v}$ (m s^{-1})	$[Al]_i$ (% abs.)[c]	$[CO_2]$ (10^{14} ml^{-1})	$\bar{T}$ (K)	k_1 (10^{-13} ml $molecule^{-1}$ s^{-1})
Reactor 3, 480 K nominal						
TF309.3	3.1	19	5	2.2 - 14	480	5.3
TF309.3	3.1	21	18	3.6 - 15	480	6.9
TF309.3	3.2	47	4	3.2 - 15	480	6.8
TF309.3	3.2	48	15	2.0 - 10	480	10.2
TA309.3	5.8	48		2.0 - 12	490	9.9
TF309.3	10	11	6	3.7 - 9.0[e]	460	5.2
TF309.3	10	21	20	0.8 - 4.1[e]	480	6.6
TF309.3	11	53	6	3.9 - 14	460	6.1
TA309.3	17	22		1.3 - 26	490	6.0
TF309.3	20	11	8	2.0 - 7.0	490	6.8
TF309.3	20	21	18	4.6 - 11	470	5.1
TF309.3	21	43	16	4.7 - 10	460	7.7
				Avg.[d]	480 ± 10	6.9 ± 1.7

TABLE I (Continued)

Mode[a]	P (Torr)[b]	$\bar{v}$ (m s^{-1})	$[Al]_i$ (% abs.)[c]	$[CO_2]$ (10^{14} ml^{-1})	$\bar{T}$ (K)	k_1 (10^{-12} ml molecule^{-1} s^{-1})
Reactor 1 (except as noted by f), 730 K nominal						
TF309.3[f]	3.8	32	3	1.9 - 10	720	1.4
TF309.3	4.3	56	5	1.0 - 6.6	800	1.9
SF309.3	3.8	78	6	0.5 - 22	710	1.9
TF309.3	3.8	80	6	0.5 - 12	720	1.5
TF309.3	11	20	3	0.5 - 2.0	780	1.8
TA309.3[f]	10	42		2.9 - 18	710	0.8
SF309.3	11	52	4	0.1 - 7.2	730	2.2
SF309.3	11	98	3	0.6 - 21	710	1.3
SA309.3	11	101		0.5 - 19	740	1.6
TA309.3[f]	19	20		0.6 - 3.3	730	2.6
SA309.3	22	35		0.1 - 10	740	1.3
SF309.3	29	25	4	0.1 - 6.8	710	1.5
TF309.3	30	52	5	2.0 - 9.0	720	1.4
				Avg.[d]	730 ± 30	1.6 ± 0.5

TABLE I (Continued)

Mode[a]	P (Torr)[b]	$\bar{v}$ ($m\ s^{-1}$)	$[Al]_i$ (% abs.)[c]	$[CO_2]$ (10^{13} ml^{-1})	$\bar{T}$ (K)	k_1 (10^{-12} ml molecule^{-1} s^{-1})
Reactor 1, 1470 K nominal						
TA309.3	3.2	26		8.3 - 16[e]	1430	8.1
SA396.2	3.5	43		2.4 - 11	1480	11
TA396.2	3.5	49		11 - 41	1470	9.6
TA309.3	3.4	88		8.2 - 28	1470	8.8
TA309.3	8.6	26		2.3 - 11	1480	7.8
SA396.2	8.6	49		1.1 - 23	1500	9.1
SF309.2	8.6	93	9	3.8 - 65	1450	4.4
SA396.2	8.6	95		4.6 - 72	1500	5.4
TA309.3	16	25		3.8 - 15	1480	6.3
SA309.3	16	25		0.4 - 26[e]	1480	7.3
SA396.2	16	48		1.3 - 24[e]	1430	12
SA396.2	16	97		1.7 - 47	1440	11
SF309.3	16	99	5	1.8 - 15	1460	8.5
TA396.2	31	50		4.0 - 45[e]	1430	7.2
SA396.2	31	50		1.5 - 38	1450	14
TA396.2	31	51		4.7 - 19	1470	11
SA396.2	31	52		1.7 - 16	1500	14
SF309.3	32	100	5	1.7 - 10	1460	6.5
				Avg.[d]	1470 ± 20	9.0 ± 2.7

TABLE I (continued)

Mode[a]	P (Torr)[b]	$\bar{v}$ (m s^{-1})	$[Al]_i$ (% abs.)[c]	$[CO_2]$ (10^{12} ml^{-1})	$\bar{T}$ (K)	k_1 (10^{-11} ml molecule^{-1} s^{-1})
Reactor 1, 1830 K nominal						
SA309.3	4.1	93		8.0 - 122	1850	3.6
SA394.4	12	10		1.4 - 12[e]	1840	6.2
SA309.3	13	15		2.5 - 21[e]	1840	2.7
SA394.4	12	25		1.6 - 34[e]	1810	3.8
SA394.4	14	90		1.0 - 570	1830	3.5
SA394.4	30	10		1.3 - 8.1	1830	3.5
TA394.4	30	10		4.7 - 13[e]	1820	5.5
SA309.3	31	14		2.3 - 34[e]	1820	3.2
SA394.4	31	25		1.0 - 14[e]	1820	2.4
SA309.3	32	47		3.5 - 56[e]	1830	3.4
				Avg.[d]	1830 ± 10	3.8 ± 1.2

a The first letter, T or S, indicates whether the CO_2 inlet nozzle was traversed or kept stationary; the second letter F or A, whether $[Al]_{rel}$ was measured in fluorescence or absorption; the number indicates the wavelength (in nm) of the Al line used.

b 1 Torr = 133.3 Pa

c % initial Al absorption is shown for the experiments in which $[Al]_{rel}$ was monitored by fluorescence; for the 310 and 1470 K experiments the 396.3 nm line was used for this absorption measurement while in the 480 and 730 K work the 309.3 nm line was used. In experiments in which $[Al]_{rel}$ was obtained by absorption the initial absorption was on the order of 50%.

d Mean and standard deviation

e In these experiments 9.56% CO_2 in Ar was used, in all other experiments undiluted CO_2.

f These experiments were carried out in Reactor 3.

FIGURE CAPTIONS

FIG. 1 Schematic of modular HTFFR (Reactor 3) used for 480 and some 730 K experiments

FIG. 2 Arrhenius plot of the measured rate coefficients grouped by temperature.

FIG. 3 Comparison of fitting functions $k_1(T)$ with the individual data points

Curve (E): Arrhenius form with T-independent pre-exponential;

Curve (E'): Arrhenius form with $T^{1/2}$ dependence of pre-exponential;

Curve (F): T^n form; Curve (G): Transition state theory form;

Curve (H): Double exponential form.

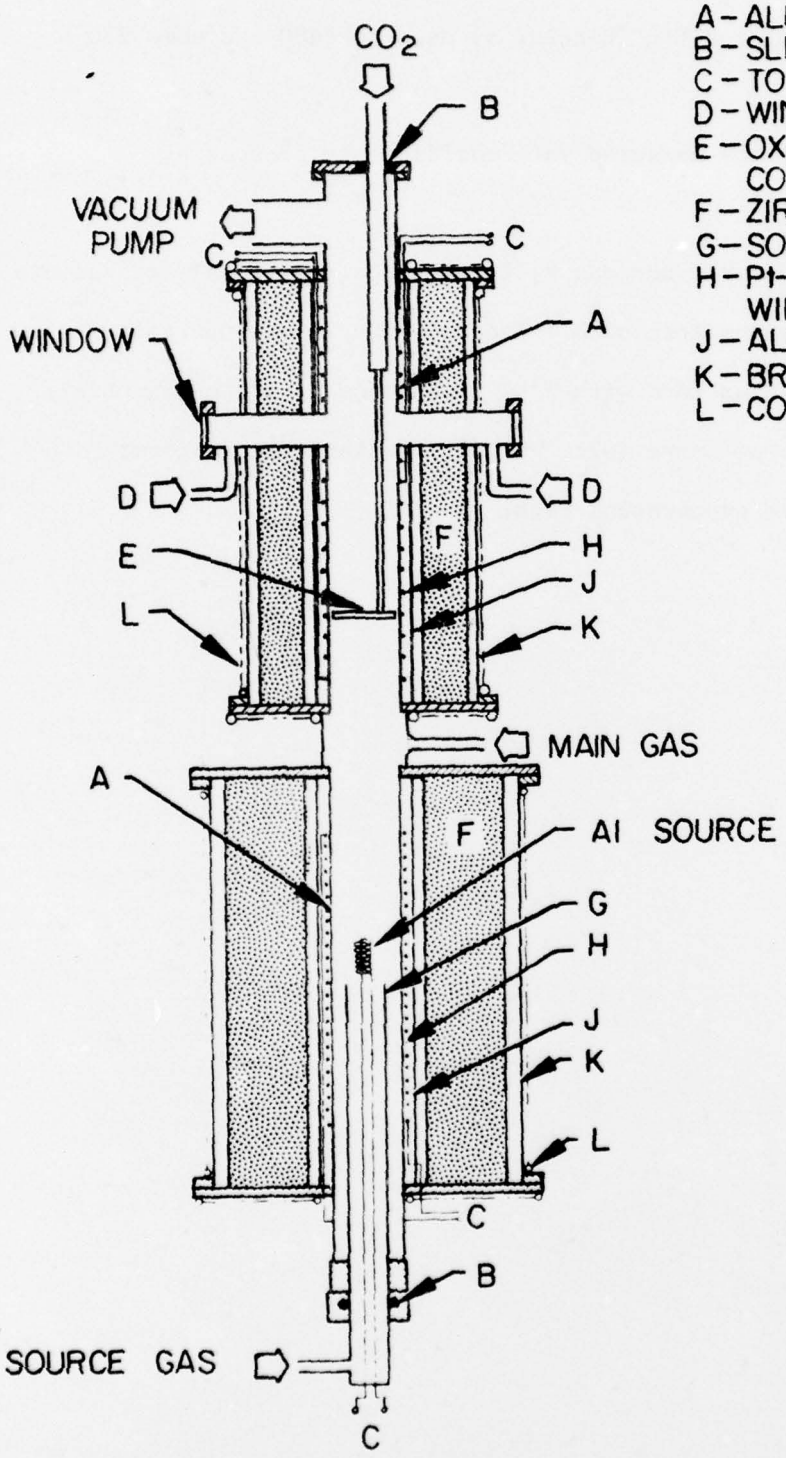

A - ALUMINA TUBE
B - SLIDING O-RING SEAL
C - TO POWER SUPPLY
D - WINDOW SWEEPER GAS
E - OXIDANT INLET and THERMO-COUPLE WELL
F - ZIRCAR INSULATION
G - SOURCE HOLDER
H - Pt-40% Rh RESISTANCE WIRE
J - ALUMINA HEAT SHIELD
K - BRASS VACUUM HOUSING
L - COOLING COIL

FIG. 1

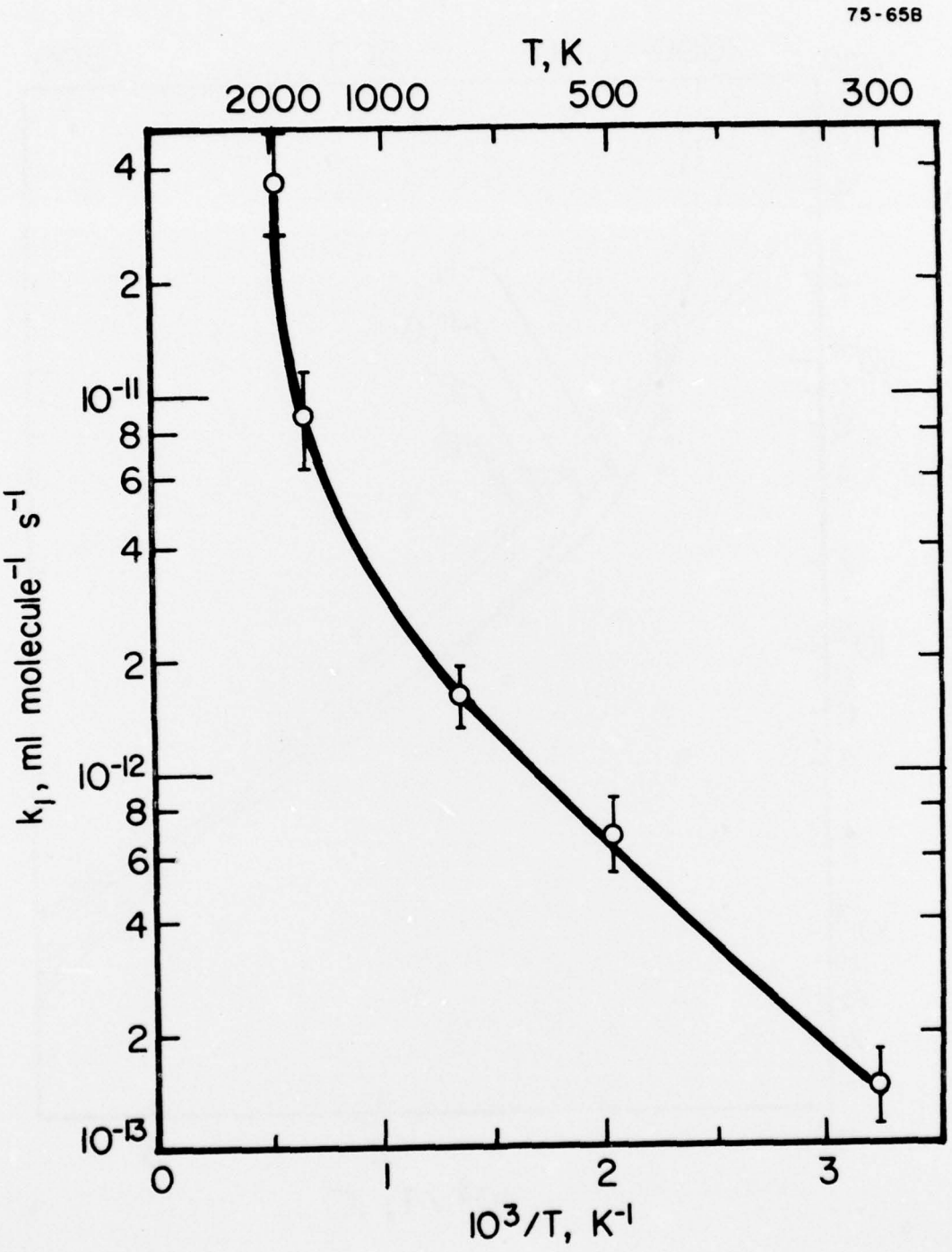
75-658
T, K
2000 1000 500 300
4
2
10^{-11}
8
6
4
2
10^{-12}
8
6
4
2
10^{-13}
k_1, ml molecule^{-1} s^{-1}
0 1 2 3
$10^3/T$, K^{-1}

FIG. 2

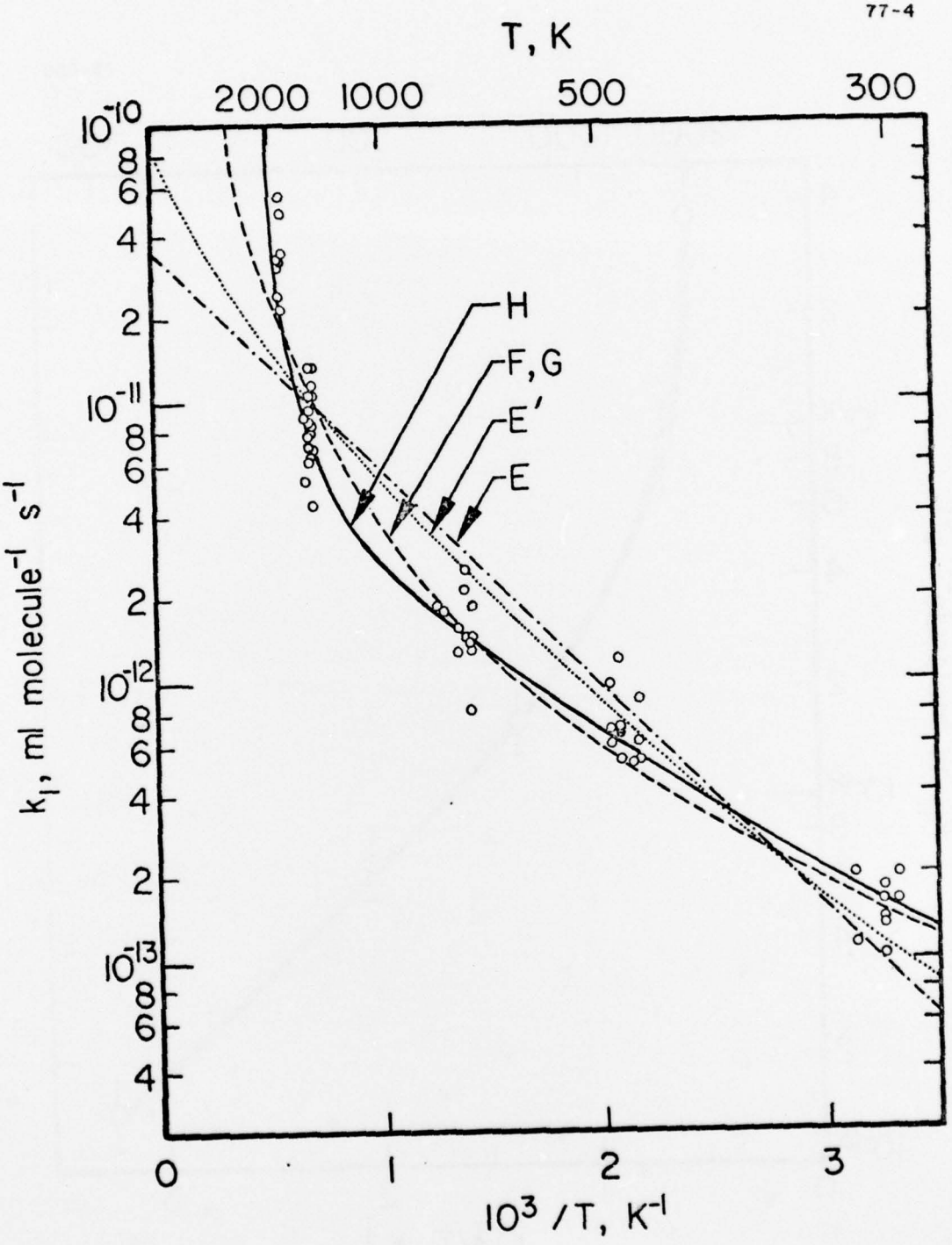
T, K
2000
1000
500
300
H
F, G
E'
E
k_1, ml molecule^{-1} s^{-1}
10^{-10}
10^{-11}
10^{-12}
10^{-13}
0
1
2
3
10^3 /T, K^{-1}

FIG. 3

DISTRIBUTION LIST

GOVERNMENT AGENCIES

1. British Embassy
   3100 Massachusetts Avenue, N.W.
   Washington, D.C. 20008
   ATTN: Mr. J. Barry Jamieson
   Propulsion Officer

2. Central Intelligence Agency
   Washington, D.C. 20505
   ATTN: CRS/ADD/Publications

3. Institute for Defense Analyses
   400 Army-Navy Drive
   Arlington, Virginia 22202
   ATTN: Dr. Hans G. Wolfhard,
   Sen. Staff

4. Defense Documentation Center
   Cameron Station
   Alexandria, Virginia 22314

5. EPA Technical Center
   Research Triangle Park
   North Carolina 27711
   ATTN: Dr. W. Herget, P-222

6. Esso Research and Engineering Company
   Government Research Laboratory
   P.O. Box 8
   Linden, New Jersey 07036
   ATTN: Dr. William F. Taylor

7. Arnold Air Force Station
   Tennessee 36389
   ATTN: AEDC (DYF)

8. Arnold Air Force Station
   Tennessee 37389
   ATTN: R.E. Smith, Jr., Chief
   T-Cells Division
   Engine Test Facility

9. Air Force Aero Propulsion Laboratory
   Wright-Patterson Air Force Base
   Ohio 45433
   ATTN: STINFO Office

10. Air Force Eastern Test Range
    MU-135
    Patrick Air Force Base
    Florida 32925
    ATTN: AFETR Technical Library

11. Air Force Office of Scientific Research
    Bolling Air Force Base, Building 410
    Washington, D.C. 20332
    ATTN: Dr. Joseph F. Masi

12. Air Force Aero Propulsion Laboratory
    Wright-Patterson AFB, Ohio 45433
    ATTN: AFAPL/TBC
    Dr. Kervyn Mach

13. Air Force Aero Propulsion Laboratory
    Wright-Patterson AFB, Ohio 45433
    ATTN: AFAPL/TBC
    Francis R. Ostdiek

14. Air Force Rocket Propulsion Laboratory
    Department of Defense
    Edwards AFB, California 93523
    ATTN: LKCG (Mr. Selph)

15. U.S. Army Air Mobility Research and
    Development Laboratory
    Eustis Directorate
    Fort Eustis, Virginia 23604
    ATTN: Propulsion Division
    (SAVDL-EU-PP)

16. U.S. Army Artillery Combat
    Developments Agency
    Fort Sill, Oklahoma 73503
    ATTN: Commanding Officer

17. U.S. Army Missile Command
    Redstone Arsenal, Alabama 35809
    ATTN: AMSMI-RR

18. U.S. Army Missile Command
    Redstone Scientific Information Center
    Redstone Arsenal, Alabama 35809
    ATTN: Chief, Document Section

19. Indiana State Library
    140 North Senate Avenue
    Indianapolis, Indiana 46204
    ATTN: Patricia Matkovic
    Reference Librarian
    % Indiana Division

20. NASA Headquarters
    600 Independence
    Washington, D.C. 20546
    ATTN: Dr. Gordon Banerian

21. NASA Headquarters
    Aeronautical Propulsion Division
    Code RL, Deputy Director
    Office of Advanced Research & Technology
    Washington, D.C. 20546
    ATTN: Mr. Nelson F. Rekos

22. NASA Ames Research Center
    Deputy Chief Aeronautics Division
    Mail Stop 27-4
    Moffett Field, California 94035
    ATTN: Mr. Edward W. Perkins

23. NASA Ames Research Center
    Aerodynamics Branch 227-8
    Moffett Field, California 94305
    ATTN: Mr. Ira R. Schwartz

24. NASA Lewis Research Center
    21000 Brookpark Road
    Cleveland, Ohio 44135
    ATTN: D. Morris, Mail Stop 60-3

25. NASA Lewis Research Center
    Hypersonic Propulsion Section
    Mail Stop 6-1
    21000 Brookpark Road
    Cleveland, Ohio 44135
    ATTN: Dr. Louis A. Povinelli

26. NASA Marshall Space Flight Center
    S&E ASTN-P
    Huntsville, Alabama 35812
    ATTN: Mr. Keith Chandler

27. National Science Foundation
    Engineering Energetics
    Engineering Division
    Washington, D.C. 20550
    ATTN: Dr. George Lee

28. National Science Foundation
    Engineering Energetics
    Engineering Division
    Washington, D.C. 20550
    ATTN: Dr. M. Ojalvo

29. National Science Foundation
    Engineering Energetics
    Engineering Division
    Washington, D.C. 20550
    ATTN: Dr. Royal Rostenbach

30. Naval Air Development Center
    Commanding Officer (AD-5)
    Warminster, Pennsylvania 18974
    ATTN: NADC Library

31. Naval Air Propulsion Test Center (R&T)
    Trenton, New Jersey 08628
    ATTN: Mr. Al Martino

32. Naval Air Systems Command
Department of the Navy
Washington, D.C. 20360
ATTN: Research Administrator
AIR 310

33. Naval Air Systems Command
Department of the Navy
Washington, D.C. 20360
ATTN: Propulsion Technology Admin.
AIR 330

34. Naval Air Systems Command
Department of the Navy
Washington, D.C. 20360
ATTN: Technical Library Division
AIR 604

35. Naval Ammunition Depot
Research and Development Department
Building 190
Crane, Indiana 47522
ATTN: Mr. B.E. Douda

36. Naval Ordnance Laboratory Commander
White Oak
Silver Springs, Maryland 20910
ATTN: Library

37. Naval Ordnance Systems Command
Department of the Navy
Washington, D.C. 20360
ATTN: ORD 0331

38. Naval Postgraduate School
Department of Aeronautics, Code 57
Monterey, California 93940
ATTN: Dr. Allen E. Fuhs

39. Naval Postgraduate School
Library (Code 2124)
Monetrey, California 93940
ATTN: Superintendent

40. Naval Postgraduate School
Monterey, California 93940
ATTN: Library (Code 0212)

41. Office of Naval Research Branch Office
1030 East Green Street
Pasadena, California 91106
ATTN: Dr. Rudolph J. Marcus

42. Office of Naval Research Branch Office
536 South Clark Street
Chicago, Illinois 60605
ATTN: Commander

43. Office of Naval Research Branch Office
495 Summer Street
Boston, Massachusetts 02210
ATTN: Commander

44. Office of Naval Research
Power Branch, Code 473
Department of the Navy
Arlington, Virginia 22217

45. Office of Naval Research
Fluid Dynamics Branch, Code 438
Department of the Navy
Washington, D.C. 22217
ATTN: Mr. Morton Cooper

46. Naval Research Lab
Code 7710
Washington, D.C. 20390
ATTN: W.W. Balwanz

47. Naval Research Laboratory Director
Washington, D.C. 20390
ATTN: Technical Information Division

48. Naval Research Laboratory Director
Washington, D.C. 20390
ATTN: Library Code 2629 (ONRL)

49. Naval Ship Research and Development Center
Annapolis Division
Annapolis, Maryland 21402
ATTN: Library, Code A214

50. Naval Ship Systems Command
Department of the Navy
Washington, D.C. 20360
ATTN: Technical Library

51. Naval Weapons Center Commander
China Lake, California 93555
ATTN: Airbreathing Propulsion Branch
Code 4583

52. Naval Weapons Center
Chemistry Division
China Lake, California 93555
ATTN: Dr. William S. McEwan
Code 605

53. Naval Weapons Center
Commander
China Lake, California 93555
ATTN: Technical Library

54. Naval Weapons Center
Code 608, Thermochemistry Group
China Lake, California 93555
ATTN: Mr. Edward W. Price, Head

55. Naval Weapons Laboratory
Dahlgren, Virginia 22448
ATTN: Technical Library

56. Naval Undersea Research and
Development Center
San Diego, California 92132
ATTN: Technical Library
Code 13110

57. Naval Underwater Systems Center
Fort Trumbull
New London, Connecticut 06320
ATTN: Technical Library

58. Naval Underwater Systems Center
Code 5B-331
Newport, Rhode Island 02840
ATTN: Dr. Robert Lazar

59. Picatinny Arsenal
Commanding Officer
Dover, New Jersey 07801
ATTN: Technical Information Library

60. State Documents Section
Exchange and Gift Division
Washington, D.C. 20540
ATTN: Library of Congress

U.S. INDUSTRIES AND LABORATORIES

61. AeroChem Research Laboratories, Inc.
P.O. Box 12
Princeton, New Jersey 08540
ATTN: Dr. Arthur Fontijn

62. AeroChem Research Laboratories, Inc.
P.O. Box 12
Princeton, New Jersey 08540
ATTN: Library

63. Aerojet Liquid Rocket Company
P.O. Box 13222
Sacramento, California 95813
ATTN: Technical Information Center

64. Aeronautical Research Association
of Princeton
50 Washington Road
Princeton, New Jersey 08540
ATTN: Dr. C. Donaldson

65. Aeroprojects, Inc.
West Chester
Pennsylvania 19380

66. The Aerospace Corporation
P.O. Box 92957
Los Angeles, California 90009
ATTN: Mr. Alexander Muraszew

67. Atlantic Research Corporation
5390 Cherokee Avenue
Alexandria, Virginia 22314
ATTN: Dr. Andrej Macek

68. Atlantic Research Corporation
5390 Cherokee Avenue
Alexandria, Virginia 22314
ATTN: Librarian

69. Atlantic Research Corporation
5390 Cherokee Avenue
Alexandria, Virginia 22314
ATTN: Dr. Kermit E. Woodcock
Manager, Propulsion

70. Avco Everett Research Laboratory
Everett, Massachusetts 02149
ATTN: Librarian

71. Avco Lycoming Corporation
550 South Main Street
Stratford, Connecticut 06497
ATTN: Mr. John W. Schrader

72. Ballistics Research Laboratory
Commanding Officer
Aberdeen Proving Ground, Maryland 21005
ATTN: Library

73. Battelle
Columbus Laboratories
505 King Avenue
Columbus, Ohio 43201
ATTN: Mr. Abbott A. Putnam
Atmospheric Chemistry &
Combustion Systems Division

74. Beech Aircraft Corporation
9709 East Central
Wichita, Kansas 67201
ATTN: William M. Byrne, Jr.

75. Bell Aerospace Company
P.O. Box 1
Buffalo, New York 14240
ATTN: Technical Library

76. Bureau of Mines
Bartlesville Energy Research Center
Box 1398
Bartlesville, Oklahoma 74003

77. Calspan Corporation
4455 Genessee Street
Buffalo, New York 14221
ATTN: Head Librarian

78. Computer Genetics Corporation
Wakefield, Massachusetts 01880
ATTN: Mr. Donald Leonard
Technical Director

79. Convair Aerospace Division
Manager of Propulsion
P.O. Box 748
Fort Worth, Texas 76101
ATTN: L. H. Schreiber

80. Detroit Diesel Allison Division
P.O. Box 894
Indianapolis, Indiana 46206
ATTN: Dr. Sanford Fleeter

81. Dynalysis of Princeton
20 Nassau Street
Princeton, New Jersey 08540
ATTN: Dr. H.J. Herring

82. Fairchild Industries
Fairchild Republic Division
Farmingdale, New York 11735
ATTN: Engineering Library

83. Flame Research, Inc.
P.O. Box 10502
Pittsburgh, Pennsylvania 15235
ATTN: Dr. John Manton

84. Forest Fire and Engineering Research
Pacific Southwest Forest & Range
Experiment Station
P.O. Box 245
Berkeley, California 94701
ATTN: Assistant Director

85. Garrett Corporation
AiResearch Manufacturing Company
Sky Harbor Airport
402 South 36th Street
Phoenix, Arizona 85034
ATTN: Mr. Aldo L. Romanin, Mgr.
Aircraft Propulsion Engine
Product Line

86. General Dynamics
Electro Dynamic Division
P.O. Box 2507
Pomona, California 91766
ATTN: Library MZ 620

87. General Dynamics
P.O. Box 748
Fort Worth, Texas 76101
ATTN: Technical Library MZ 2246

88. General Electric Company
AEG Technical Information Center
Mail Drop N-32, Building 700
Cincinnati, Ohio 45215
ATTN: J.J. Brady

89. General Electric Company
SPO-Bldg, 174AE
1000 Western Avenue
West Lynn, Massachusetts 01910
ATTN: Mr. W. Bruce Gist

90. General Electric Space Sciences Lab
Valley Forge Space Technology Center
Room M-9144
P.O. Box 8555
Philadelphia, Pennsylvania 19101
ATTN: Dr. Theodore Baurer

91. General Motors Corporation
Detroit Diesel Allison Division
P.O. Box 894
Indianapolis, Indiana 46206
ATTN: Mr. P.C. Tram

92. General Motors Technical Center
Passenger Car Turbine Development
General Motors Engineering Staff
Warren, Michigan 48090
ATTN: T.F. Nagey, Director

93. Grumman Aerospace Corporation
Manager Space Vehicle Development
Bethpage, New York 11714
ATTN: Mr. O.S. Williams

94. Mr. Daniel L. Harshman
11131 Embassy Drive
Cincinnati, Ohio 45240

95. Hercules Incorporated
Allegany Ballistics Laboratory
P.O. Box 210
Cumberland, Maryland 21502
ATTN: Mrs. Louise S. Derrick
Librarian

96. Hercules Incorporated
P.O. Box 98
Magna, Utah 84044
ATTN: Library 100-H

97. LTV Vought Aeronautics Company
Flight Technology, Project Engineer
P.O. Box 5907
Dallas, Texas 75222
ATTN: Mr. James C. Utterback

98. Lockheed Aircraft Corporation
Lockheed Missiles and Space Company
Huntsville, Alabama 35804
ATTN: John M. Banefield
Supervisor Propulsion

99. Lockheed-Georgia Company
Dept. 72-47, Zone 259
Marietta, Georgia 30060
ATTN: William A. French

100. Lockheed Missiles and Space Company
3251 Hanover Street
Palo Alto, California 94304
ATTN: Palo Alto Library 52-52

101. Lockheed Propulsion Company
Scientific and Technical Library
P.O. Box 111
Redlands, California 92373
ATTN: Head Librarian

102. Los Alamos Scientific Laboratory
P.O. Box 1663
Los Alamos, New Mexico 87544
ATTN: J. Arthur Freed

103. The Marquardt Company
CCI Aerospace Corporation
16555 Saticoy Street
Van Nuys, California 91409
ATTN: Library

104. Martin-Marietta Corporation
P.O. Box 179
Denver, Colorado 90201
ATTN: Research Library 6617

105. Martin-Marietta Corporation
Orlando Division
P.O. Box 5837
Orlando, Florida 32805
ATTN: Engineering Library, mp-30

106. McDonnell Aircraft Company
P.O. Box 516
St. Louis, Missouri 63166
ATTN: Research & Engineering Library
Dept. 218 - Bldg. 101

107. McDonnell Douglas Corporation
Project Propulsion Engineer
Dept. 243, Bldg. 66, Level 25
P.O. Box 516
St. Louis, Missouri 63166
ATTN: Mr. William C. Paterson

108. McDonnell Douglas Astronautics Company
5301 Bolsa Avenue
Huntington Beach, California 92647
ATTN: A3-328 Technical Library

109. Nielsen Engineering and Research, Inc.
510 Clyde Avenue
Mountain View, California 94040
ATTN: Dr. Jack N. Nielsen

110. Northrop Corporation
Ventura Division
1515 Rancho Conejo Boulevard
Newbury Park, California 91230
ATTN: Technical Information Center

111. Mr. J. Richard Perrin
16261 Darcia Avenue
Encino, California 91316

112. Philco-Ford Corporation
Aeronutronic Division
Ford Road
Newport Beach, California 92663
ATTN: Technical Information Center

113. Pratt and Whitney Aircraft
Project Engineer, Advanced
Military System
Engineering Department - 2B
East Hartford, Connecticut 06108
ATTN: Mr. Donald S. Rudolph

114. Pratt and Whitney Aircraft Division
United Aircraft Company
400 South Main Street
East Hartford, Connecticut 06108
ATTN: Mr. Dana B. Waring
Manager-Product Technology

115. Pratt and Whitney Aircraft
Program Manager, Advanced
Military Engineer
Engineering Department - 2B
East Hartford, Connecticut 06108
ATTN: Dr. Robert I. Strough

116. Pratt and Whitney Aircraft
Florida Research and Development Company
P.O. Box 2691
West Palm Beach, Florida 33402
ATTN: Mr. William R. Alley
Chief of Applied Research

117. Rocket Research Corporation
11441 Willow Road
Redmond, Washington 98052
ATTN: Thomas A. Groudle

118. Rocketdyne Division
North American Rockwell
6633 Canoga Avenue
Canoga Park, California 91304
ATTN: Technical Information Center
D 596-108

119. Sandia Laboratories
P.O. Box 969
Livermore, California 94550
ATTN: Dr. Dan Hartley, Div. 8115

120. Sandia Laboratories
Livermore, California 94550
ATTN: Robert Gallagher

121. Sandia Laboratories
P.O. Box 5800
Albuquerque, New Mexico 87115
ATTN: Technical Library, 3141

122. Solar
2200 Pacific Highway
San Diego, California 92112
ATTN: Librarian

123. Standard Oil Company (Indiana)
P.O. Box 400
Naperville, Illinois 60540
ATTN: R. E. Pritz

124. Stauffer Chemical Company
Richmond, California 94802
ATTN: Dr. J. H. Morgenthaler

125. Teledyne CAE
1330 Laskey Road
Toledo, Ohio 43601
ATTN: Technical Library

126. TRW Systems
One Space Park
Redondo Beach, California 90278
ATTN: Mr. F.E. Fendell (R1/1004)

127. TRW Systems Group
One Space Park
Bldg. 0-1 Room 2080
Redondo Beach, California 90278
ATTN: Mr. Donald H. Lee Manager

128. United Technologies Research Center
East Hartford, Connecticut 06108
ATTN: Librarian

129. Valley Forge Sapce Technology Center
P.O. Box 8555
Philadelphia, Pennsylvania 19101
ATTN: Dr. Bert Zauderer

130. Vought Missiles and Space Company
P.O. Box 6267
Dallas, Texas 75222
ATTN: Library - 3-41000

131. Boston College
Department of Chemistry
Chestnut Hill, Massachusetts 02167
ATTN: Rev. Donald MacLean, S.J.
Associate Professor

132. Brown University
Division of Engineering
Box D
Providence, Rhode Island 02912
ATTN: Dr. R. A. Dobbins

133. California Institute of Technology
Department of Chemical Engineering
Pasadena, California 91109
ATTN: Professor W. H. Corcoran

134. California Institute of Technology
Jet Propulsion Laboratory
4800 Oak Grove Drive
Pasadena, California 91103
ATTN: Library

135. University of California, San Diego
Dept. of Engineering Physics
P.O. Box 109
La Jolla, California 92037
ATTN: Professor S.S. Penner

136. University of California
School of Engineering and
Applied Science
7513 Boelter Hall
Los Angeles, California 90024
ATTN: Engineering Reports Group

137. University of California
Lawrence Radiation Laboratory
P.O. Box 808
Livermore, California 94550
ATTN: Technical Information Dept. L-3

138. University of California
General Library
Berkeley, California 94720
ATTN: Documents Department

139. Case Western Reserve University
10900 Euclid Avenue
Cleveland, Ohio 44106
ATTN: Sears Library - Reports
Department

140. Case Western Reserve University
Division of Fluid Thermal and
Aerospace Sciences
Cleveland, Ohio 44106
ATTN: Professor Eli Reshotko

141. Colorado State University
Engineering Research Center
Fort Collins, Colorado 80521
ATTN: Mr. V. A. Sandborn

142. The University of Connecticut
Department of Mechanical Engineering
U-139
Storrs, Connecticut 06268
ATTN: Professor E. K. Dabora

143. Cooper Union
School of Engineering and Science
Cooper Square
New York, New York 10003
ATTN: Dr. Wallace Chintz
Associate Professor of ME

144. Cornell University
Department of Chemistry
Ithaca, New York 14850
ATTN: Professor Simon H. Bauer

145. Franklin Institute Research Laboratories
Philadelphia, Pennsylvania 19103
ATTN: Dr. G.P. Wachtell

146. George Washington University
Washington, D.C. 20052
ATTN: Dr. Robert Goulard
Dept. of Civil, Mechanical and
Environmental Engineering

147. George Washington University Library
Washington, D.C. 20006
ATTN: Reports Section

148. Georgia Institute of Technology
Atlanta, Georgia 30332
ATTN: Price Gilbert Memorial Library

149. Georgia Institute of Technology
School of Aerospace Engineering
Atlanta, Georgia 30332
ATTN: Dr. Ben T. Zinn

150. University of Illinois
Department of Energy Engineering
Box 4348
Chicago, Illinois 60680
ATTN: Professor Paul H. Chung

151. University of Illinois
College of Engineering
Department of Energy Engineering
Chicago, Illinois 60680
ATTN: Dr. D. S. Hacker

152. The Johns Hopkins University
Applied Physics Laboratory
Johns Hopkins Road
Laurel, Maryland 20810
ATTN: Chemical Propulsion
Information Agency

153. The Johns Hopkins University
Applied Physics Laboratory
Johns Hopkins Road
Laurel, Maryland 20810
ATTN: Document Librarian

154. The Johns Hopkins University
Applied Physics Laboratory
Johns Hopkins Road
Laurel, Maryland 20810
ATTN: Dr. A. A. Westenberg

155: University of Kentucky
Department of Mechanical Engineering
Lexington, Kentucky 40506
ATTN: Dr. Robert E. Peck

156. Massachusetts Institute of Technology
Department of Chemical Engineering
Cambridge, Massachusetts 02139
ATTN: Dr. Jack B. Howard

157. Massachusetts Institute of Technology
Libraries, Room 14 E-210
Cambridge, Massachusetts 02139
ATTN: Technical Reports

158. Massachusetts Institute of Technology
Room 10-408
Cambridge, Massachusetts 02139
ATTN: Engineering Technical Reports

159. Massachusetts Institute of Technology
Dept. of Mechanical Engineering
Room 3-350
Cambridge, Massachusetts 02139
ATTN: Dr. M. Cardillo

160. Massachusetts Institute of Technology
Dept. of Mechanical Engineering
Room 3-246
Cambridge, Massachusetts 02139
ATTN: Professor James Fay

161. Midwest Research Institute
425 Volker Boulevard
Kansas City, Missouri 64100
ATTN: Dr. T. A. Milne

162. New Mexico State University
Dept. of Mechanical Engineering
Box 3450
Las Cruces, New Mexico 88003
ATTN: Dr. Dennis M. Zallen

163. New York Institute of Technology
Wheatley Road
Old Westbury, New York 11568
ATTN: Dr. Fox

164. University of North Carolina
Periodicals and Serials Division
Drawer 870 Library
Chapel Hill, North Carolina 27514
ATTN: Mr. Stephen Berk

165. University of Notre Dame
Serials Record
Memorial Library
Notre Dame, Indiana 46556
ATTN: B. McIntosh

166. University of Notre Dame
College of Engineering
Notre Dame, Indiana 46556
ATTN: Dr. Stuart T. McComas
Assistant Dean for Research
and Special Projects

167. Ohio State University
Dept. of Chemical Engineering
140 West 19th Avenue
Columbus, Ohio 43210
ATTN: Dr. Robert S. Brodkey

168. The Pennsylvania State University
Room 207, Old Main Building
University Park, Pennsylvania 16802
ATTN: Office of Vice President
for Research

169. Princeton University
Dept. of Aerospace and Mechanical
Sciences
James Forrestal Campus
Princeton, New Jersey 08540
ATTN: Dr. Martin Summerfield

170. Princeton University
James Forrestal Campus Library
P.O. Box 710
Princeton, New Jersey 08540
ATTN: V. N. Simosko, Librarian

171. Rice University
Welch Professor of Chemistry
Houston, Texas 77001
ATTN: Dr. Joseph L. Franklin

172. University of Rochester
Dept. of Chemical Engineering
Rochester, New York 14627
ATTN: Dr. John R. Ferron

173. Stanford University
Dept. of Aeronautics and Astronautics
Stanford, California 94305
ATTN: Dr. Walter G. Vincenti

174. State University of New York - Buffalo
Dept. of Mechanical Engineering
228 Parker Engineering Building
Buffalo, New York 14214
ATTN: Dr. George Rudinger

175. Stevens Institute of Technology
Department of Mechanical Engineering
Castle Point Station
Hoboken, New Jersey 07030
ATTN: Professor Fred Sisto

176. University of Virginia
Department of Aerospace Engineering
School of Engineering and Applied Science
Charlottesville, Virginia 22901
ATTN: Dr. John E. Scott

177. University of Virginia
Science/Technology Information Center
Charlottesville, Virginia 22901
ATTN: Dr. Richard H. Austin

178. Yale University
Mason Laboratory
9 Hillhouse Avenue
New Haven, Connecticut 06520
ATTN: Professor Peter P. Wegener

FOREIGN INSTITUTIONS

179. A/S Kongsberg Vaapenfabrikk
Gas Turbine Division
3601 Konsber, NORWAY
ATTN: R.E. Stanley
Senior Aerodynamicist

180. Conservatoire National des Arts
et Metiers
292, Rue Saint'Martin
75141 Paris Cedex 03, FRANCE
ATTN: Professor J. Gossee
Chaire de Thermique

181. DFVLR-Forschungszentrum Gottingen
Institut Fur Stromungsmechanik
Abteilung Theoretische Gashynamik
D-3400 Gottingen
Bunsenstrabe 10, GERMANY
ATTN: Professor Klaus Oswatitsch

182. Ecole Royale Militaire
30 Avenue de la Resaissance
Bruxelles B-1040, BELGIUM
ATTN: Professor Emile Tits

183. Fysisch Laboratorium
Fijksuniversiteit Utrecht
Sorbonnelaan, Utrecht,
THE NETHERLANDS
ATTN: Dr. F. Van der Valk

184. Imperial College
Department of Chemical Engineering
London SW7, ENGLAND
ATTN: Professor F. J. Weinberg

185. Imperial College of Science
and Technology
Department of Mechanical Engineering
Exhibition Road
London, SW7, ENGLAND
ATTN: Professor Gaydon

186. Imperial College of Science
and Technology
Department of Mechanical Engineering
Exhibition Road
London SW7, ENGLAND
ATTN: D. B. Spalding

187/1 Laboratoire de Mecanique des Fluides
36, Route de Dardilly, 36
B.P. No. 17
69130 Ecully, FRANCE
ATTN: G. Assassa

187/2 Laboratoire de Mecanique des Fluides
Ecole Centrale Lyonnaise
36, Route de Dardilly
69130 Ecully, FRANCE
ATTN: Dr. K. Papiliou

188. Ministry of Defense
Main Building, Room 2165
Whitehall Gardens
London SW1, ENGLAND
ATTN: Mr. L.D. Nicholson ED, idc
Vice Controller of Aircraft
Procurement Executive

189. Mitglied des Vorstands der Fried
Krumpp CmbH
43 Essen, Altendorferstrabe 103
GERMANY
ATTN: Professor Dr.-Ing.
Wilhelm Dettmering

190. National Aerospace (NLR)
Voorsterweg 31
Noord-Oost-Polder-Emmelord
THE NETHERLANDS
ATTN: Mr. F. Jaarsma

191. National Research Council
Division of Mechanical Engineering
Montreal Road, Ottawa
Ontario, CANADA KIA OR6
ATTN: Dr. R.B. Whyte

192. Nissan Motor Co., LTD.
3-5-1, Momoi, Suginami-Ku
Tokyo, JAPAN 167
ATTN: Dr. Y. Toda

193. Norweigian Defense Research Establishment
Superintendent NDRE
P.O. Box 25
2007 Kjeller, NORWAY
ATTN: Mr. T. Krog

194. ONERA
Energie and Propulsion
29 Avenue de la Division Leclure
92 Chatillon sous Bagneux, FRANCE
ATTN: Mr. M. Barrere

195. ONERA
Energie and Propulsion
29 Avenue de la Division Leclure
92 Chatillon sous Bagneux, FRANCE
ATTN: Mr. J. Fabri

196. ONERA
Energie and Propulsion
29 Avenue de la Division Leclure
92 Chatillon sous Bagneux, FRANCE
ATTN: Mr. Viaud

197. ONERA-DED
External Relations and Documentation
Department
29, Avenue de la Division Leclure
92320 Chatillon, sous Bagneux, FRANCE
ATTN: Mr. M. Salmon

198. Orta Dogu Teknik Universities
Mechanical Engineering Department
Ankara, TURKEY
ATTN: Professor H. Sezgen

199. Queen Mary College
Department of Mechanical Engineering
Thile Eld Road
London El, ENGLAND
ATTN: Professor M. W. Thring

200. Rolls-Royce (1971) Limited
Derby Engine Division
P.O. Box 31
Derby DE2 8BJ
London, ENGLAND
ATTN: C. Freeman, Installation
Research Department

201. Rome University
Via Bradano 28
00199 Rome, ITALY
ATTN: Professor Gaetano Salvatore

202. Sener
Departamentao de Investigation
Km. 22.500 de la antigua carretera
Madrid - Barcelona, SPAIN
ATTN: Mr. J. T. Diez Roche

203. Service Technique Aeronautique Moteurs
4 Avenue de la Parte d'Issy
75753 Paris Cedex 15, FRANCE
ATTN: Mr. M. Pianko, Ing. en chef

204. The University of Sheffield
Dept. of Chemical Engineering
and Fuel Technology
Mappin Street, Sheffield S1 3JD
ENGLAND
ATTN: Dr. Norman Chigier

205. Sophia University
Science and Engineering Faculty
Kioi 7 Tokyo-Chiyoda JAPAN 102
ATTN: Professor M. Susuki

206. The University of Sydney
Dept. of Mechanical Engineering
N.S.W. 2006
Sydney, AUSTRALIA
ATTN: Professor R. W. Bilger

207. Technical University of Denmark
Fluid Mechanics Department
Building 404 2800 Lyngby
DK-DENMARK
ATTN: Professor K. Refslund

208. University of Leeds
Leeds, ENGLAND
ATTN: Professor Dixon-Lewis

209. Universite de Poitiers Laboratoire
D'energetique et de Detonique
(L.A. au C.N.R.S. No. 193)
ENSMA - 86034 Poitiers, FRANCE
ATTN: Professor N. Manson

210. University of Tokyo
Department of Reaction Chemistry
Faculty of Engineering
Bunkyo-ku
Tokyo, JAPAN 113
ATTN: Professor T. Hikita

211. Vrije Universiteit Brussel
Fac. Toeg. Wetenshch.
A. Buyllaan 105
1050 Brussels, BELGIUM
ATTN: Ch. Hirsch

PROJECT SQUID CONTRACTORS
1975-76 and 1976-77 (New)

212. AeroChem Research Laboratory, Inc.
Reaction Kinetics Group
P.O. Box 12
Princeton, New Jersey 08540
ATTN: Dr. Arthur Fontijn

213. Aeronautical Research Associates of
Princeton, Inc.
P.O. Box 2229
50 Washington Road
Princeton, New Jersey 08540
ATTN: Dr. Ashok K. Varma

214. California Institute of Technology
Div. of Engineering and
Applied Science
Mail Stop 205-50
Pasadena, California 91109
ATTN: Dr. Anatol Roshko

215. Case Western Reserve University
Div. of Fluid, Thermal and Aerospace
Sciences
Cleveland, Ohio 44106
ATTN: Dr. J.S. T'ien

216. Colorado State University
Engineering Research Center
Foothills Campus
Fort Collins, Colorado 80521
ATTN: Dr. Willy Z. Sadeh

217. General Electric Company
Corporate Research and Development
P.O. Box 8
Schenectady, New York 12301
ATTN: Dr. Marshall Lapp

218. Massachusetts Institute of Technology
Chemistry Department, Room 6-123
77 Massachusetts Avenue
Cambridge, Massachusetts 02139
ATTN: Dr. John Ross

219. Michigan State University
Department of Mechanical Engineering
East Lansing, Michigan 48824
ATTN: Dr. John Foss

220. Pennsylvania State University
Applied Research Laboratory
University Park, Pennsylvania 16802
ATTN: Dr. Edgar P. Bruce

221. Polytechnic Institute of New York
Department of Aerospace Engineering
and Applied Mechanics
Farmingdale, New York 11735
ATTN: Dr. Samuel Lederman

222. Southern Methodist University
Thermal and Fluid Sciences Center
Institute of Technology
Dallas, Texas 75275
ATTN: Dr. Roger L. Simpson

223. Stanford University
Mechanical Engineering Department
Stanford, California 94305
ATTN: Dr. James P. Johnston

224. Stanford University
Mechanical Engineering Department
Stanford, California 94305
ATTN: Dr. S. J. Kline

225. Stanford University
Mechanical Engineering Department
Stanford, California 94305
ATTN: Dr. Sidney Self

226. TRW Systems
Engineering Sciences Laboratory
One Space Park
Redondo Beach, California 90278
ATTN: Dr. J. E. Broadwell

227. United Technologies Research Center
400 Main Street
East Hartford, Connecticut 06108
ATTN: Mr. Franklin O. Carta

228. United Technologies REsearch Center
400 Main Street
East Hartford, Connecticut 06108
ATTN: Dr. Alan C. Eckbreth

229. University of California - San Diego
Department of Aerospace and
Mechanical Engineering
La Jolla, California 92037
ATTN: Dr. Paul Libby

230. University of Colorado
Department of Aerospace
Engineering Sciences
Boulder, Colorado 80304
ATTN: Dr. Mahinder S. Uberoi

231. University of Michigan
Department of Aerospace Engineering
Ann Arbor, Michigan 48105
ATTN: Dr. T. C. Adamson, Jr.

232. University of Michigan
Department of Aerospace Engineering
Ann Arbor, Michigan 48105
ATTN: Dr. Martin Sichel

233. University of Missouri - Columbia
Department of Chemistry
Columbia, Missouri 65201
ATTN: Dr. Anthony Dean

234. University of Southern California
Department of Aerospace Engineering
University Park
Los Angeles, California 90007
ATTN: Dr. F. K. Browand

235. University of Washington
Department of Mechanical Engineering
Seattle, Washington 98195
ATTN: Dr. F.B. Gessner

236. Virginia Polytechnic Institute and
State University
Mechanical Engineering Department
Blacksburg, Virginia 24601
ATTN: Dr. Walter F. O'Brien, Jr.

237. Virginia Polytechnic Institute and
State University
Mechanical Engineering Department
Blacksburg, Virginia 24061
ATTN: Dr. Hal L. Moses

238. Yale University
Engineering and Applied Science
Mason Laboratory
New Haven, Connecticut 06520
ATTN: Dr. John B. Fenn

PURDUE UNIVERSITY

239. School of Aeronautics and Astronautics
Grissom Hall
West Lafayette, Indiana 47907
ATTN: Library

240. School of Mechanical Engineering
Mechanical Engineering Building
West Lafayette, Indiana 47907
ATTN: Library

241-250. Purdue University Advisors

UNCLASSIFIED

SECURITY CLASSIFICATION OF THIS PAGE *(When Data Entered)*

REPORT DOCUMENTATION PAGE

READ INSTRUCTIONS BEFORE COMPLETING FORM

1. REPORT NUMBER

2. GOVT ACCESSION NO.

3. RECIPIENT'S CATALOG NUMBER

4. TITLE *(and Subtitle)*

HTFFR KINETICS STUDIES OF Al + CO_2 → AlO + CO FROM 300 to 1800 K, A NON-ARRHENIUS REACTION

5. TYPE OF REPORT & PERIOD COVERED

6. PERFORMING ORG. REPORT NUMBER

AeroChem TP-353

7. AUTHOR(s)

Arthur Fontijn
William Felder

8. CONTRACT OR GRANT NUMBER(s)

9. PERFORMING ORGANIZATION NAME AND ADDRESS

AeroChem Research Laboratories, Inc.
P.O. Box 12
Princeton, NJ 08540

10. PROGRAM ELEMENT, PROJECT, TASK AREA & WORK UNIT NUMBERS

11. CONTROLLING OFFICE NAME AND ADDRESS

12. REPORT DATE

March 1977

13. NUMBER OF PAGES

44

14. MONITORING AGENCY NAME & ADDRESS *(if different from Controlling Office)*

15. SECURITY CLASS. *(of this report)*

Unclassified

15a. DECLASSIFICATION/DOWNGRADING SCHEDULE

16. DISTRIBUTION STATEMENT *(of this Report)*

17. DISTRIBUTION STATEMENT *(of the abstract entered in Block 20, if different from Report)*

18. SUPPLEMENTARY NOTES

19. KEY WORDS *(Continue on reverse side if necessary and identify by block number)*

Reaction Kinetics
Combustion
Al (metal atoms)
CO_2

20. ABSTRACT *(Continue on reverse side if necessary and identify by block number)*

High-temperature fast-flow reactors (HTFFR) were used to obtain the rate coefficients, k_1 (and their accuracies), for the reaction Al + CO_2 → AlO + CO. At 310, 480, 730, 1470, and 1830 K, k_1 is found to be $(1.5 \pm 0.6) \times 10^{-13}$, $(6.9 \pm 2.7) \times 10^{-13}$, $(1.6 \pm 0.7) \times 10^{-12}$, $(9.0 \pm 3.8) \times 10^{-12}$ and $(3.8 \pm 1.5) \times 10^{-11}$, respectively (all in ml molecule^{-1} s^{-1} units). For this temperature range $k_1(T)$ may be expressed by the curve fitting equation

$$k_1(T) = 2.5 \times 10^{-13} T^{1/2} \exp(-1030/T) + 1.4 \times 10^{-9} T^{1/2} \exp(-14{,}000/T)$$

DD FORM 1 JAN 73 1473 EDITION OF 1 NOV 65 IS OBSOLETE

UNCLASSIFIED

SECURITY CLASSIFICATION OF THIS PAGE *(When Data Entered)*

(Block 20 continued)

The data also indicate a wall-oxidation process of zeroth order in $[CO_2]$ with a γ_{Al} of 10^{-3} to 10^{-2}, not measurably dependent on T. Factors affecting the accuracy of the measurements are discussed. Over the 310-730 K range $k_1(T)$ obeys an Arrhenius expression, with an activation energy of 2.6 ± 1.3 kcal $mole^{-1}$, which implies $D(Al-O) \geq 122$ kcal $mole^{-1}$. Above 730 K, $k_1(T)$ increases much more rapidly with T. This behavor cannot be described on the basis of simple transition state theory alone; the most probable additional factors involved are the opening of a second reaction channel leading to $AlO(A^2\Pi)$ and preferential reaction of Al with CO_2 in bending modes.